2002

Evaluation of the hydrocarbon potential in low-salinity shaly sand

Fnu Kurniawan

Louisiana State University and Agricultural and Mechanical College

Recommended Citation

Kurniawan, Fnu, "Evaluation of the hydrocarbon potential in low-salinity shaly sand" (2002). *LSU Master's Theses*. 2311.
https://repository.lsu.edu/gradschool_theses/2311

EVALUATION OF THE HYDROCARBON POTENTIAL IN LOW-SALINITY SHALY SAND

A Thesis

Submitted to the Graduate Faculty of the
Louisiana State University and
Agricultural and Mechanical College
In partial fulfillment of the
Requirements for the degree of
Master of Science
In Petroleum Engineering

in

The Department of Petroleum Engineering

by
Kurniawan
B.S., Institute of Technology Bandung (Indonesia), 1996
May 2002

ACKNOWLEDGEMENTS

At this opportunity the author wishes to express special gratitude and sincere appreciation to Dr. Zaki Bassiouni, Chairman of the Petroleum Engineering Department, for his valuable guidance and genuine interest as research advisor and chairman of the examination committee. Deep appreciation is also extended to other members of the committee, Dr. Dandina N. Rao and Dr. Chistopher D. White, for their support and constructive suggestions. Additional gratitude is also extended to Dr. John McMullan and Dr. John R. smith for their suggestions and assistance.

In addition, appreciation is extended to Paradigm Geophysical for providing a very useful well-log analysis software (Geolog6) to complete this study.

Finally, the author is also indebted to the Petroleum Engineering Department, for providing the financial support, which made this study possible.

TABLE OF CONTENTS

LIST OF TABLES

LIST OF FIGURES

ABSTRACT

This research utilizes reservoir data from an oilfield in Indonesia, which is characterized by shaly sand and low salinity formation water. Both low salinity and shaliness reduce the resistivity contrast between oil and water. The aim of this research was to build a comprehensive interpretation algorithm to evaluate the shaly-sand reservoir in a low salinity formation water using limited well log data.

Shaly-sand interpretation is still evolving with numerous researchers conducting investigations of the clay minerals effect on rock conductivity through theoretical and experimental approach. These investigations can be loosely divided into either Fractional Shale Volume models or the Cation Exchange Capacity (clay-type) models.

This research emphasizes the Cation Exchange Capacity models. Cation Exchange Capacity (CEC) is essentially a reflection of the specific surface area of clay minerals, which causes additional conductivity in shaly-sands. The modified Silva-Bassiouni model was used to interpret shaly sand formations. This model is based on the dual water concept, however it considers that the counter-ion conductivity can be represented by an equivalent sodium chloride solution. Therefore, this method eliminates the requirement for actual CEC measurements from cores. The Shale Volume based Simandoux and Indonesia models were used for comparison. The results from the Archie clean sand model were also discussed. The model was evaluated using actual production and well test data.

The modified Silva-Bassiouni model was found to yield superior estimates of cation exchange capacity and fluid saturations in the reservoirs.

CHAPTER 1

INTRODUCTION

The interpretation of Shaly-Sands log data has long been a challenging problem. As a result, there are more than 30 shaly-sand interpretation models, which have been developed in the last 50 years[1].Interpretation difficulties arise whenever the portions of clay minerals in a shaly-sand formation is high. In Indonesian formation particularly, the limit is 30%[2]. These clay minerals contribute to the increase of the overall conductivity. In a large quantity, their conductivity becomes as important as the conductivity of the formation water[3].

The well-known Archie formula for calculating water saturation in a shale-free reservoir is expressed as[4]:

$$\mathbf{S_w}^{\mathbf{n}} = \frac{\mathbf{C_t}}{\phi^{\mathbf{m}}.\mathbf{C_w}} \tag{1.1a}$$

or as:

$$\mathbf{S_w}^{\mathbf{n}} = \frac{\mathbf{R_w}}{\phi^{\mathbf{m}}.\mathbf{R_t}} \tag{1.1b}$$

where:

$\mathbf{S_w}$ = formation water saturation, fraction

$\mathbf{C_t}$ = rock conductivity, mho/m

$\mathbf{C_w}$ = brine conductivity, mho/m

$\mathbf{R_w}$ = resistivity of formation water, ohm/m

$\mathbf{R_t}$ = resistivity of formation rock, ohm/m

ϕ = porosity, fraction

n = saturation exponent

m = cementation exponent

Archie formula has been widely used by many log analyst especially when dealing with clean sand reservoir. This empirical formula provided the early basis of the quantitative petrophysical reservoir evaluation. Practically, there are several ways to estimate the formation water resistivity (Rw) such as from applying equation 1.1b to nearby water sand, from water sample measurements, and from the Spontaneous Potential (SP) log. The formation rock resistivity (Rt) is usually obtained from deep resistivity log reading such as deep Induction or deep Lateralog. Meanwhile the porosity data (ϕ) can be estimated from several types of porosity logs, for instance Density, Neutron, or Sonic log. Finally, the saturation exponent (**n**) and cementation exponent (**m**) are estimate from core data analysis or from prior experience with local formation characteristics.

In evaluating shaly-sand reservoir, Archie formula may give a misleading result. This is because Archie formula assumes that the formation water is the only electrically conductive material in the formation. The shale effect on various log responses depends on the type, the amount, and the way it is distributed in the formation[5].

Shale can be distributed in sandstone reservoirs in three possible ways as shown in **Figure 1.1** they are[5]: (1) laminar shale, where shale can exist in the form of laminae between layers of clean sand; (2) structural shale, where shale can exist as grains or nodules within the formation matrix; and (3) dispersed shale, where shale can be dispersed throughout the sand, partially filling the intergranular interstices, or can be coating the sand grains. All this form can occur simultaneously in the same formation. Each form can affect the amount of rock porosity by creating a layer of closely bound surface water on the shale particle.

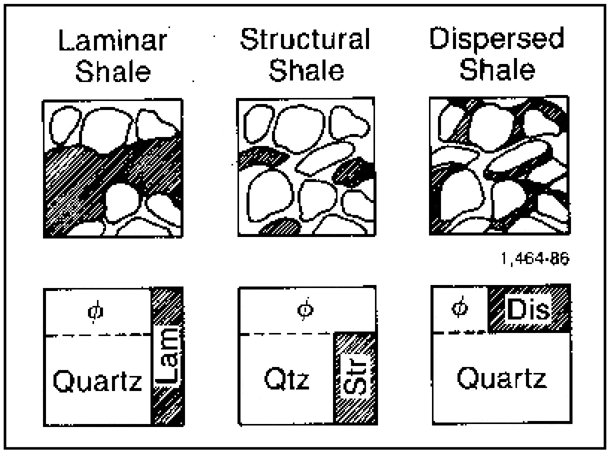

Figure 1.1 - Different ways of shale distribution in formation.

The effect of shaliness on electrical conductivity is illustrated in **Figure 1.2.** The figure shows the conductivity of water-saturated sandstone (**C_o**) as a function of the water conductivity (**C_w**). The straight line of gradient 1/F represents the application of Archie's equation on clean reservoir rock fully saturated with brine. However, in the other rock with same effective porosity but some of the rock matrix is replaced by shale, the straight line is displaced upward with respect to the original clean sand line. This increase of conductivity is because of the shaliness effect and known as the excess conductivity (C_{excess}).

Based on their different approach and concept, the shaly-sand models that currently available can be divided into two main groups: fractional volume of shale (Vsh) group and Cation Exchange Capacity (CEC) group.

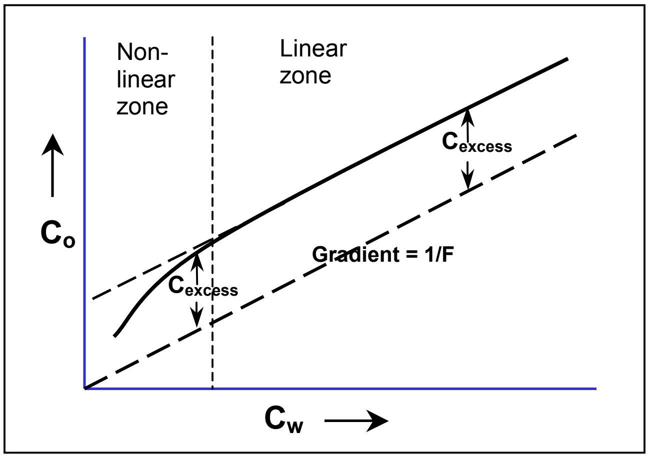

Figure 1.2 - The variation of C_o and C_w as a result of shaliness effect.

1.1 Volume of Shale (Vsh) Models

The Vsh quantity is defined as the volume of wetted shale per unit volume of reservoir rock. Wetted shale mean that the space occupied by the water confined to the shale, known as bound water, should be taken into account to determine the total porosity.

These models are applicable to logging data without the encumbrance of a core sample calibration of the shale related parameter. However, they have also lead to certain misunderstanding and misusing because they are used beyond its limitation.

The Simandoux model[6] that was introduced in 1963 is still widely used to some extent. This model basically use porosity from Density-Neutron data and shale fraction determined from GR, SP, or other shale indicator. This equation is only covering the linear zone of the schematic shown in **Figure 1.2**. However, to accommodate the non-linear zone, several Vsh models have also been introduced by various log-analyst. For instance the "Indonesia formula" proposed by Poupon and Leveaux[2] in1971. This equation was originally developed for used in Indonesia, but later was found applicable in some other area. It is important to note that each model can only give a partial correlation to the rock conductivity data zone, i.e., Simandoux and Poupon-Leveaux relationship accommodate linear and no-linear zone, respectively[1]. The correction made in one zone will result in a mismatch of another zone. This problem shows a major limitation of using the Vsh models to interpret shaly-sand reservoir because no universally accepted equations exist.

Another major disadvantage of Vsh models is that they do not take into account the mode of distribution or the composition of different clay types. The variation of clay mineralogy can result in different shale effects for the same volume of shale fraction (Vsh). Further improved models, which take into account the shortage in Vsh model such as geometry and electrochemistry of mineral-electrolyte interfaces, start to become more reliable models in shaly-sand interpretation. These models can be classified into one group known as cation exchange capacity models.

1.2 Cation Exchange Capacity Models

Crystalline clay platelets are negatively charged as the result of ion substitutions in the lattice and broken bonds at the edge. Sodium cations (Na^+) is the typical charge-balancing cations. These cations are held in suspension close to the clay surface when the clay is in contact with saline solution. As a result, the Cl^- anions in the solution will be repelled from the clay surface.

As shown in **Figure 1.3**, a mono-layered of adsorbed water exists directly on the clay surface. To sufficiently balance the negative platelet charge, another layer of hydrated Na+ ions is also present.

The concentration of sodium cations can be measured in term of cation exchange capacity (CEC), expressed in milliequivalents per gram of dry clay. For practical purpose Q_v, cation exchange capacity per unit of pore volume, is usually used. This is the source of the excess conductivity shown in **Figure 1.2**.

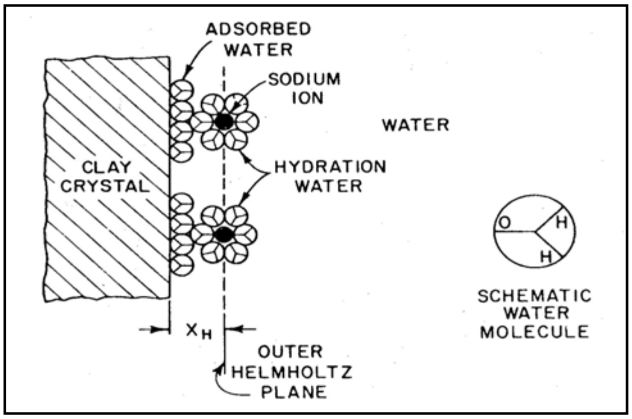

Figure 1.3 - Model of water bound to a clay surface (courtesy of Schlumberger)

In 1968, Waxman and Smits, based on extensive laboratory work and theoretical study, proposed a saturation-resistivity relationship for shaly formation using the assumption that cation conduction and the conduction of normal sodium chloride act independently in the pore space, resulting parallel conduction paths. This model can be expressed by[7]:

$$\mathbf{C_t = \frac{S_w{}^n . C_w}{F^*} + \frac{B . Q_v . S_w{}^{n-1}}{F^*}} \tag{1.2}$$

where:

C_t = rock conductivity

S_w = water saturation

ne = saturation exponent for shaly formations

B = equivalent conductance of clay counterions

C_w = water conductivity

F* = formation factor of the interconnected porosity

According to this model, a shaly formation behaves like a clean formation of the same porosity, tortuosity, and fluid saturation, except the water appears to be more conductive than its bulk salinity. In other words, it says that the increase of apparent water conductivity is dependent on the presence of counter-ion. A Dual-Water model[8] based on this premise was introduced.

The Dual-Water model[8] is a modification of Waxman-Smits equation by taking into account the exclusion of anions from the double-layer. It represents the counterion conductivity restricted to the bound water, where counterion reside and the free water, which is found at a distance away from clay surface. This model says that apparent water conductivity will depend on the relative volumes of clay bound water and free water. Dual-water equation is given by:

$$C_t = \frac{1}{F_o} S_w^{n} \left[\beta \, . \, Q_v' + (1 - 0.28 \, . \, \alpha \, . \, Q_v') . \, C_w \right] \tag{1.3}$$

where:

β = equivalent conductivity of sodium counter-ions

α = expansion factor of diffuse layer

F_o = idealized formation factor

Q_v' is defined as:

$$Q_v' = \frac{Q_v}{S_w} \tag{1.4}$$

Another model, which based on the dual-water concept was later proposed by Silva and Bassiouni in 1985. Although this model is based on dual-water concept it differs from the previous one. It considers that the equivalent counter-ion conductivity is related to conductivity of an equivalent sodium chloride solution. Therefore, it is a function of temperature and the conductivity of the free water. This model can be expressed as follow[9]:

$$C_t = \frac{{S_w}^n}{F_e} [C_{eq}' \,.\, Q_v' + (1 - v_{fdl}')\, C_w] \tag{1.5}$$

where:

C_{eq} = counter-ion conductivity

v_{fdl} = fractional volume of the double layer

F_e = equivalent formation factor

Compared to the previous two models, Silva-Bassiouni model has practical advantages since it does not need clay counter-ions data measured from core analysis because it can be represented by sodium chloride solution. This approach is applicable to the real field condition since the conductivity data of sodium chloride solutions can be obtained at high temperatures as in field condition.

This conductivity model together with another membrane potential model, which also proposed by Silva and Bassiouni in 1987, will be used to construct a reliable algorithm to calculate the water saturation in shaly-sand reservoir using the data from one of the Central Sumatra oil field. Since both models are expressed in term of the cation exchange capacity of clay, $\mathbf{Q_v}$, and the free electrolyte conductivity, $\mathbf{C_w}$, so in water bearing zone these two unknown parameter can be determined simultaneously.

CHAPTER 2

CONDUCTIVITY AND MEMBRANE POTENTIAL MODELS

2.1 Silva-Bassiouni Conductivity Model

Silva and Bassiouni[9] introduced a new conductivity model for shaly-sand. This model treats the equivalent counter-ion conductivity as that of an equivalent sodium chloride solution. It is assumed that the conductive behavior of a shaly-sand corresponds to that of a clean sand of the same porosity that contains water with effective conductivity, C_{we}. The equation is given below:

$$\mathbf{C_{we} = C_{cl} .\ v_{fdl} + (1\text{-}v_{fdl}).\ C_w} \tag{2.1}$$

where $\mathbf{C_w}$ and $\mathbf{v_{fdl}}$ are, respectively, the conductivity of free electrolyte and the fractional volume occupied by double layer. The conductivity of exchange cations associated with clay, $\mathbf{C_{cl}}$, can be defined as:

$$\mathbf{C_{cl} = C_{eq}\ .\ n_{eq}} \tag{2.2}$$

where $\mathbf{C_{eq}}$ is the equivalent counter-ion conductivity. The concentration of clay counter-ion, $\mathbf{n_{eq}}$, can be expressed in terms of the counter-ion concentration per total pore volume, $\mathbf{Q_v}$, as:

$$\mathbf{n_{eq} = \frac{Q_v}{v_{fdl}}} \tag{2.3}$$

Because the proposed shaly-sand conductivity model simulate the expression of clean sand, the total conductivity of a rock fully saturated with water is defined by:

$$\mathbf{C_o = \frac{C_{we}}{F_e}} \tag{2.4}$$

substitution of equations (2.1) and (2.2) into equation (2.4) result in:

$$\mathbf{C_o = \frac{1}{F_e}\,[\,C_{eq}\,.\,n_{eq}\,.\,v_{fdl} + (1\text{-}v_{fdl}).\,C_w]} \tag{2.5}$$

Where $\mathbf{F_e}$ is the formation factor of an equivalent clean sand formation with the same total porosity, ϕ_T, that can be expressed as:

$$\mathbf{F_e = \phi_T^{\ -m}} \tag{2.6}$$

where **m** is the cementation exponent.

In the condition where $\mathbf{C_w}$ and $\mathbf{Q_v}$ are unknown, S-B model requires the estimation of the fractional volume of the double layer, $\mathbf{v_{fdl}}$. Juhasz[10] proposed the equation for $\mathbf{v_{fdl}}$ as:

$$\mathbf{v_{fdl} = \left(\frac{0.084}{C_w} + 0.22\right).Q_v} \tag{2.7}$$

S-B model also requires the estimation of the equivalent counter-ion conductivity, $\mathbf{C_{eq}}$. Since the equivalent counter-ion conductivity is treated as the equivalent sodium chloride solution, Silva, P (1986) provided the equation of concentration, $\mathbf{n_{eq}}$, and conductivity, $\mathbf{C_{eq}}$, which also based on the sodium chloride solution as:

$$\mathbf{n_{eq} = \frac{3.571}{\left(\sqrt{\alpha} - 0.188\right)^2}} \tag{2.8}$$

$$\mathbf{C_{eq} = \frac{C_{eq}'}{f_g\,.F_{(ne)}}} \tag{2.9}$$

where:

$\mathbf{C_{eq}'}$ = equivalent sodium chloride solution

$\mathbf{f_g}$ = geometric correction factor

F(ne) = empirical correction factor

According to Silva[11], at temperature of 25° C :

C_{eq}' can be expressed as:

$$C_{eq}' = \frac{12.645 + 7.6725\sqrt{n_{eq}}}{1 + 1.3164 . n_{eq}} \tag{2.10}$$

f_g is given by:

$$f_g = \alpha^{1/\eta} \tag{2.11}$$

where α is the expansion factor of the double layer and η is an empirical function of α defined as:

$$\eta = 0.6696 + 1.1796.\alpha - 0.14426.\alpha^2 \tag{2.12}$$

F(ne) can be presented as:

$$F(ne) = 1.0 \; ; \qquad \text{for } n_{eq} \leq 0.5 \text{ mol/l} \tag{2.13}$$

$$F(ne) = 1 + 3.83\times10^{-2}(n_{eq}-0.5) + 1.761\times10^{-2}(n_{eq}-0.5)^2 \; ; \quad \text{for neq} > 0.5 \text{ mol/l}$$

2.2 Silva-Bassiouni Membrane Potential Model

As extension of the previous conductivity model, Silva and Bassiouni[12] developed a model to predict the membrane potentials in shaly formation. This model a modification of the basic expression for the membrane potential, **Em**, in shaly sand obtained by Smits[13] and reported by Thomas[14] in the form:

$$Em = \frac{-2.R.T}{F} \int_{m2}^{m1} T_{Na}^{+} . \, d\ln(m.\gamma\pm) \tag{2.14}$$

where:

m_1 and **m_2** = molal concentration of two solution separated by the membrane, mol/kg H_2O

R = universal gas constant

T = absolute temperature, ^{o}K

F = Faraday constant

$\mathbf{T_{Na}}^{+}$= sodium transport number, and

$\gamma\pm$ = mean activity coefficient

At high salinity solution, Silva-Bassiouni observed that Smits membrane potentials model deviate from the experimental data. The deviations are believed the result of different transport properties between the solution outside the rock and those of the equivalent fluid occupying the pore space. S-B introduced an empirical correction factor, τ, to account for the differences between the actual transport properties of the system and those of the outside solution. Accordingly, the membrane potentials is given by:

$$\mathbf{E_m = \frac{-2.R.T}{F} \int_{m2}^{m1} \tau.\ T_{Na}^{+}.\ dln(m.\gamma\pm)} \qquad (2.15)$$

where:

$$\tau\ \mathbf{= 1 - \frac{0.28Q_v}{C_w}(C_w - C_{wN})}\ ;\ \text{for } \mathbf{C_w} > \mathbf{C_{wN}} \qquad (2.16)$$

$$\tau\ \mathbf{= 1\ ;} \qquad \text{for } \mathbf{C_w} \leq \mathbf{C_{wN}} \qquad (2.17)$$

where at 25°C, $\mathbf{C_{wN}}$ is equal to16.61 mho/m

2.2.1 Determination of Transport Number in Shaly Sands, $\mathbf{T_{Na}}^{+}$

Cation transport number, $\mathbf{T_{Na}}^{+}$, is a representation of the fraction of electrical charges transported by cations during the conduction of the electrical current. With the assumption of the same ionic mobility during conduction, cation transport number can expressed as:

$$T_{Na}^{+} = \frac{\textbf{Current transported by } Na^{+}}{\textbf{Total Current}} \qquad (2.18)$$

In developing the expression for T_{Na}^{+}, Silva and Bassiouni were using the same assumption used by smits where the current carried by the clay counter-ions is parallel to that carried by the solution saturating the pore space. Assuming equal composition and ionic mobility, according to S-B, the transport number in shaly sands can be expressed as:

$$T_{Na}^{+} = \frac{C_{eq}.Q_v + t_{Na}^{hf}.(1 - v_{fdl}).C_w}{C_{eq}.Q_v + (1 - v_{fdl}).C_w} \qquad (2.19)$$

Where t_{Na}^{hf} is the sodium's Hittorf transport number that is known as the motion of ions relative to that of water. Substitute equation (2.19) to equation (2.14), yield the membrane potential equation:

$$E_m = \frac{-2.R.T}{F} \int_{m2}^{m1} \left[\frac{C_{eq}.Q_v + t_{Na}^{hf}.(1 - v_{fdl}).C_w}{C_{eq}.Q_v + (1 - v_{fdl}).C_w} \right] d\ln(m.\gamma\pm) \qquad (2.20)$$

2.2.2 Determination of Hittorf Transport Numbers, t_{Na}^{hf}

Stokes[15], based on the Fouss-Onsager theory of conductance, tried to derive a theoretical expression to approximate the Hittorf transport numbers. For NaCl slolution at 25°C, the Stoke equation is given by:

$$t_{Na}^{hf} = \frac{50.1 + 55.402\sqrt{n}}{126.45 + 155.726\sqrt{n}} \qquad (2.21)$$

where **n** is the electrolyte concentration in molar units, and at the same condition the molal concentration, **m**, of NaCl solution can be calculated as[16]:

$$\mathbf{m} = \frac{\mathbf{n x 10^3}}{\mathbf{9.8986x10^2 + 41.839n^{0.95} - 58.448n}} \tag{2.22}$$

2.2.3 Determination of Mean Activity Coefficient, $\gamma\pm$

The Debye-Hückel theoretical expression for the mean activity coefficient for the NaCl solution at 25°C is given by[15]:

$$\log \gamma\pm^{298} = \frac{-0.5115\sqrt{n}}{1+1.3065\sqrt{n}} - 1.75\log a_A - \log(1-0.027m) \tag{2.23}$$

where:

$$a_A = 9.9948x10^{-1} - 3.059x10^{-2}\, m - 1.5075x10^{-3}\, m^2 \tag{2.24}$$

where **m** is the electrolyte concentration in molal units.

2.2.4 Solving the Membrane Potential

The membrane potential equation (2.20) can be solved using the procedures suggested by Thomas[14] based on the relationships between the main variables and the electrolyte concentration:

1. Divide the concentration interval, **m**, into 100 subinterval points **m**(i).
2. For each **m**(i), the corresponding molarity **n**(i) is calculated by a trial-and-error procedure using equation (2.23).
3. The magnitudes of C_{eq}, v_{fdl}, t_{Na}^{hf}, $\gamma\pm$, and C_w are evaluated for each concentration subinterval, and each T_{Na}^{+}(i) is computed.
4. Multiply the result by 51.38, the value of the constant 2RT/F at 25°C.
5. The final result is then taken as the magnitude of the membrane potential.

This procedure is repeated for each case and for each concentration interval.

2.3 LSU Model

Although S-B models is a reliable models to express the resistivity behavior and membrane potential of a shaly sand, the use of some empirical parameters such as $\mathbf{f_g}$, $\mathbf{F_{(ne)}}$, and τ which can not be adapted to the high temperature condition, have created some limitations in the application of S-B models to field condition.

A new modification of S-B model by Lau[16,17,18] to eliminate the use of empirically derived correction factor is known as the LSU model. The modification is based on electrochemical properties of sodium chloride solutions and experimental observation. This model has further extended the application to temperature more than 25°C.

2.3.1 Conductivity Model

According to S-B model, the concentration of clay counter-ion, $\mathbf{n_{eq}}$, is assumed to be independent of $\mathbf{Q_v}$, and only a function of the free electrolyte concentration as shown in equation (2.8). To satisfy this assumption, an empirically determined correction factor, $\mathbf{f_g}$, was introduced so that the curve fitting can be improved. On the other hand, LSU model assumes that the counter-ion concentration is a function of both $\mathbf{Q_v}$ and the free electrolyte concentration so that the need of $\mathbf{f_g}$ can be eliminated. Therefore, LSU model use equation (2.3) by Waxman and Smits[7] to calculate $\mathbf{n_{eq}}$. At temperature higher that 25°C the expression becomes:

$$\mathbf{n_{eq}} = \frac{\mathbf{Q_v}}{\mathbf{v_{fdl}}} \frac{\mathbf{T_a}}{\mathbf{298}} \tag{2.25}$$

where $\mathbf{T_a}$ is the absolute temperature, °K.

For sodium chloride solutions at 25°C, S-B model expressed the equivalent counter-ion conductivity, $\mathbf{C_{eq}}$, as shown in equation (2.9). This model utilized the empirically determined correction factor, $\mathbf{F_{(ne)}}$, to address the ionic interactions at moderate and high concentration. LSU model eliminate the use of $\mathbf{F_{(ne)}}$ by using an analytical expression for $\mathbf{C_{eq}}$ from published experimental data[18]:

$$\ln(C_{eq}) = -58.84 - 0.1026n_{eq} - 0.787\ln(n_{eq}) - 0.0216T_a + 11.85\ln(T_a) \tag{2.26}$$

According to LSU model, fractional volume occupied by the double layer, $\mathbf{v_{fdl}}$ is expressed as:

$$v_{fdl} = (0.28 - 0.0344 \ln (T/25)) \,.\, f_{dl} \,.\, Q_v \tag{2.27}$$

where:

$$f_{dl} = \sqrt{\frac{T_a}{X_H^{\ 2}.B_o^{\ 2}.n.298}} \tag{2.28}$$

$$X_H = 6.18\ \text{Å}$$

$$B_o = 0.3248 + 1.5108\times10^{-4}T + 8.935\times10^{-7}T^2 \tag{2.29}$$

$$\ln(n) = 68.1 - 13.58\ln(T_a) + 0.0229T_a + 1.1851\ln(C_w) + 0.00467C_w \tag{2.30}$$

2.3.2 Membrane Potential Model

LSU model modify the basic expression of the membrane potential in shaly-sands obtained by Smits[13] and reported by Thomas[14] shown in equation (2.14) to become:

$$E_m = \frac{-2.R.T}{F}\int_{m2}^{m1}\left[\frac{C_{eq}.Q_v + t_{Na}^{\ +}.(1-v_{fdl}).C_w}{C_{eq}.Q_v + (1-v_{fdl}).C_w}\right] d\ln(m.\gamma\pm) \tag{2.31}$$

where $\mathbf{t_{Na}^{+}}$ the transport number of electrolyte corrected for the transport of water.

The expression of Hittorf transport number of NaCl solution at 25°C as shown in equation (2.21) is reliable only when the concentration is below 0.3 mol/l. In the condition where NaCl solution has a concentration of greater than 0.3 mol/l, Hittorf transport number ($\mathbf{t_{Na}^{hf}}$) is obtained by analyzing some experimental data from several sources[17]. The result for the concentration between 0.25 and 4.0 mol/l is given as:

$$\mathbf{t_{Na}^{hf} = -0.009\ ln(n) + 0.366} \tag{2.32}$$

LSU model also introduced the used of water transport number ($\mathbf{t_w}$) to improve the membrane potential calculation, especially when the ions are hydrated in the aqueous solutions at moderate and high concentrations[18]. It can be written as a function of $\mathbf{Q_v}$ and free water molar concentration:

$$\mathbf{t_w = t_{fw}\ .\ Q_v} \tag{2.33}$$

where:

$$\mathbf{t_{fw} = -0.07\ ln(n) + 0.98\ ; \qquad for\ n < 0.7} \tag{2.34a}$$

$$\mathbf{t_{fw} = -0.006n^3 - 0.052n^2 - 0.1626n + 0.251\ ; \quad for\ n \geq 0.7} \tag{2.34b}$$

2.3.3 THE SP MODEL

According to LSU model the SP log response in mainly the result of electrochemical potential rather than electrokinetic. Since the electrokinetic effects are considered small, it will be neglected. In front of a permeable zone, SP log response can be expressed as[19]

$$\mathbf{SP = Em_{sh} - Em_{ss}} \tag{2.35}$$

where $\mathbf{Em_{sh}}$ and $\mathbf{Em_{ss}}$ is the electrochemical potential of shale and sand, respectively. In term of transport numbers, this model in given as:

$$\mathbf{SP} = \frac{-2.R.T}{F}\int_{m2}^{m1} (T_{Na}{}^{sh} - T_{Na}{}^{ss})\, d\ln(m.\gamma\pm) \qquad (2.36)$$

where $\mathbf{T_{Na}{}^{sh}}$ and $\mathbf{T_{Na}{}^{ss}}$ is the sodium transport number in shale and sand, respectively.

Applying the general expression of the sodium transport number ($\mathbf{T_{Na}}$**),** the equation (2.36) becomes:

$$\mathbf{SP} = \frac{-2.R.T}{F}\int_{m2}^{m1} m_{eff}\, d\ln(m.\gamma\pm) \qquad (2.37)$$

$$+\ \frac{2.R.T}{F}\int_{m2}^{m1}\left[\frac{C_{eq}.n_{eq}.v_{fdl} + t_{Na}{}^{+}.(1-v_{fdl}).C_w}{C_{eq}.n_{eq}.v_{fdl} + (1-v_{fdl}).C_w}\right] d\ln(m.\gamma\pm)$$

where $\mathbf{m_{eff}}$ is the membrane efficiency. In a perfect or ideal shale membrane, only sodium ions will transport the current. Therefore the membrane is assigned as 100% membrane efficiency. In a less perfect or non-ideal membrane where cloride ions will also contribute to the conductivity across the shale, the membrane efficiency will be less than 100%. This membrane efficiency, $\mathbf{m_{eff}}$, is an empirical determined factor that equivalent to $\mathbf{T_{Na}{}^{sh}}$.

Membrane efficiency ($\mathbf{m_{eff}}$), $\gamma\pm$ and $\mathbf{t_{Na}{}^{+}}$ can be expressed as function of $\mathbf{Q_v}$ and $\mathbf{C_w}$. The expressions will be discussed hereafter.

In order to determine the value of $\mathbf{m_{eff}}$, equations (2.35) and (2.5) are re-arranged to become:

$$\mathbf{m_{eff}} = \frac{-F}{2.R.T}\,\frac{(SP + Em_{ss})}{\int_{m2}^{m1} d\ln(m\gamma\pm)} \qquad (2.38)$$

and

$$C_o.F_e = \frac{C_{eq}.n_{eq}.v_{fdl} + (1 - v_{fdl})C_w}{T_{Na}{}^{ss}} \tag{2.39}$$

There are three unknown in both equation, namely $\mathbf{Q_v}$, $\mathbf{C_w}$, and $\mathbf{m_{eff}}$. The value of Qv is zero if clean sand is present, so $\mathbf{m_{eff}}$ can be calculated simultaneously using both equations. Otherwise, $\mathbf{m_{eff}}$ value can be determined using trial and error method on the same equations.

The relation between mean activity coefficient, $\gamma\pm$, and $\mathbf{C_w}$ is given as:

$$\log(\gamma\pm) = \log(\gamma\pm^{298}) + 0.5Y.L_{298} - 0.5Z.J_{298} \tag{2.40}$$

where the calculation of mean activity coefficient at 25^0C,$\gamma\pm^{298}$**,** is shown in equation (2.23) and equation (2.24), the rest are given as:

$$Y = \frac{298.15 - T_a}{8.3147(298.15)2.3026(T_a)} \tag{2.41}$$

$$Z = 298.15\,Y - \frac{1}{8.3147}\log\left(\frac{T_a}{298.15}\right) \tag{2.42}$$

$$L_{298} = \frac{2878.6\sqrt{m}}{1+\sqrt{m}} - 3182.8m + 986.5\sqrt{m^3} \tag{2.43}$$

$$J_{298} = \frac{43.5\sqrt{m}}{1+\sqrt{m}} + 72m - 20.36\sqrt{m^3} \tag{2.44}$$

where for sodium chloride solutions the molality, **m**, can be calculated using the relation with the molarity, **n** as:

$$\ln(m) = 1.5054 + 1.0142\ln(n) + 0.272\ln(T_a) \tag{2.45}$$

The sodium chloride transport number, $\mathbf{t_{Na}{}^{+}}$ can be associated to $\mathbf{Q_v}$ and $\mathbf{C_w}$ through the given equation:

$$t_{Na}{}^{+} = t_{Na}{}^{hf} + t_w \tag{2.46}$$

where:

$$\ln(t_{Na}^{hf}) = -2.5089 - 1.8038x10^{-2}.\ln(m) + 0.2647.\ln(T_a) - 1.4176x10^{-5} . T_a.m) \tag{2.47}$$

and

$$t_w = 0.053m-0.43+(0.196\ln(m)+0.1244).Q_v \text{ ; for } m \leq 1.0 \tag{2.48}$$

$$t_w = 0.036m^{1.1} - 0.04377 + 0.04Qv \text{ ; for } m > 1.0 \tag{2.49}$$

In water bearing sand the value of C_o and **SP** can be obtained from wireline logs. Consequently, it is possible to calculate the value of Q_v and C_w simultaneously since both conductivity and spontaneous potential can be expressed exclusively as function of Q_v and C_w.

CHAPTER 3

FIELD APPLICATION

3.1 Field Description

JR field was discovered in 1973 and has been producing since then. It is located in Central Sumatra Basin, Indonesia. As shown in **Figure 3.1**, there are 3 oil-bearing formations in the JR field: X, Y and Z. The Z formation contributes 80% of the overall JR field oil production. Z formation is characterized by thick layer of well-developed stacked-channel sand that has better reservoir quality such as porosity and permeability compared to the other two. X and Y formation have lower reservoir quality due to the occurrence of clay minerals. Between those two formations, Y formation is often being under estimated because of its higher shaliness and low resistivity. Several production tests from different wells indicated the presence of hydrocarbon in some intervals of Y formation. The shale effect in the reservoir rock with low salinity formation water has created a complication in the interpretation process. In the current approach, many interpretations models were used because it was difficult to find a unique model that gives reliable results.

The LSU model[18] will be tested to determine whether this model is applicable to the typical reservoir characteristics in JR field. The result will be then compared to other models that are frequently used in this area. For discussion purpose, Archie model that was designed for use in clean sand formation will also be used to evaluate the same shaly sand interval beside other models such as: Simandoux Model and Poupon-Leveaux “Indonesia” Model. The results will then be validated using production test result from wells that has perforation interval in Y formation.

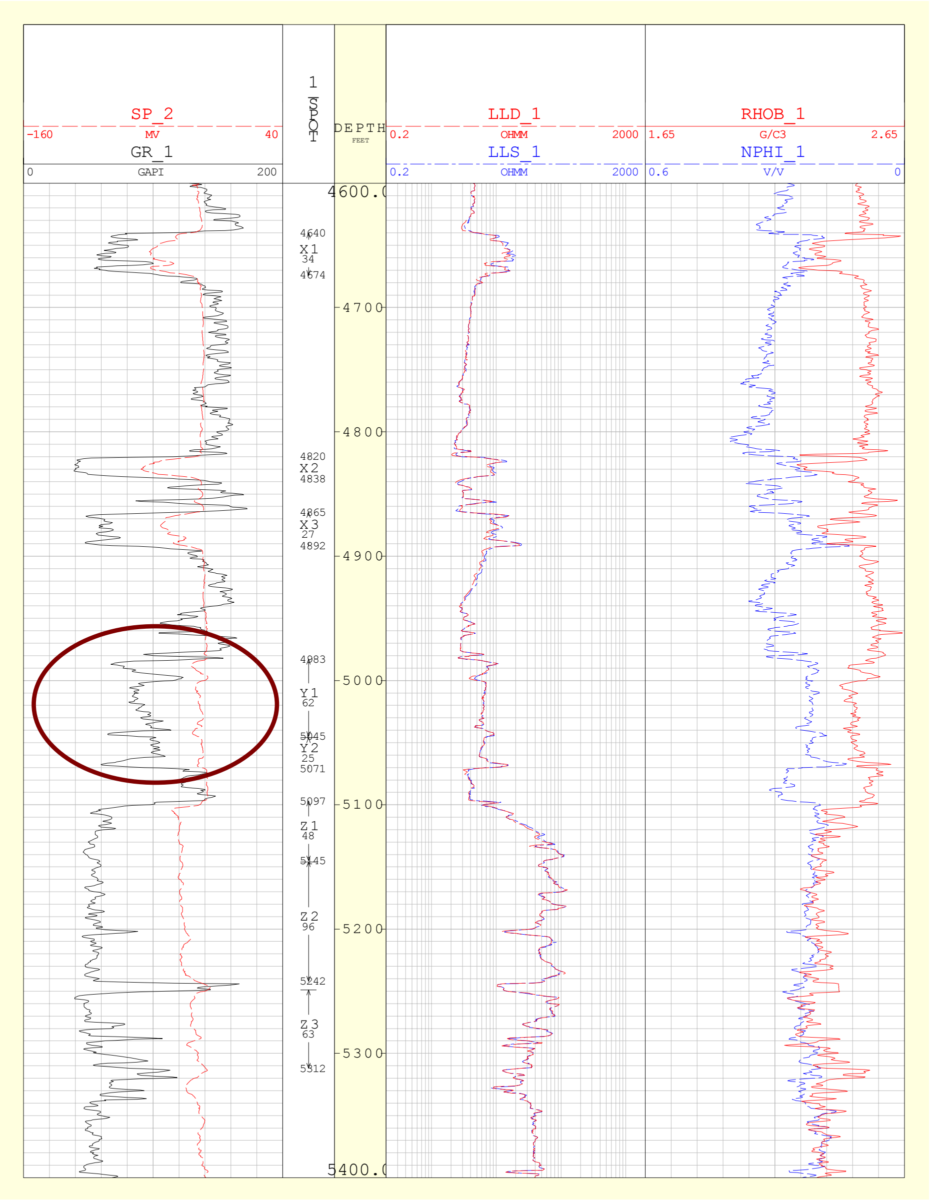

Figure 3.1 – Typical log curves of three oil-bearing formations in JR field

Data are available from 27 wells in JR field. Most of them have the basic log curves: Gamma Ray (GR), Spontaneous Potential (SP), Resistivity (Deep and Shallow), and Density (RHOB). Few wells have additional curves: Sonic (DT), Neutron (NPHI), and Micro Resistivity (MSFL). There are also other useful data such as water analysis, core analysis, and production test results.

3.2 Archie Model

Archie,[4] using experimental studies of clean formations came to an empirical relationship to calculate the water saturation of a hydrocarbon-bearing zone when an obvious water-bearing zone of the same porosity and water salinity is close by. The relation is given as:

$$S_w = \sqrt[n]{\frac{a.R_w}{\phi^m.R_t}} \qquad (3.1)$$

where:

S_w = water saturation, fraction

n = saturation exponent

a = cementation factor

m = cementation exponent

ϕ = porosity, fraction

R_w = formation-water resistivity, ohmm

R_t = invasion corrected deep resistivity, ohmm

3.3 Simandoux Model

Simandoux[6] in 1963 published his saturation model, which initially gained a wide acceptance. This saturation model is based on resistivity, density and neutron logs data. The model as shown in chapter one, is expressed as:

$$C_t = \frac{C_w.S_w^{\ n}}{F_e} + V_{sh}.\,C_{sh} \qquad (3.1)$$

In different form and for sandstone reservoir, this equation can be expressed as:

$$S_w = \frac{0.4.R_w}{\phi_e^2}\left[\sqrt{\frac{5.\phi_e^2}{R_w.R_t}+\left(\frac{V_{sh}}{R_{sh}}\right)}-\frac{V_{sh}}{R_{sh}}\right] \quad (3.2)$$

Where:

V_{sh} = shale volume, fraction

R_{sh} = deep resistivity reading in adjacent shale, ohmm

ϕ_e = effective porosity, fraction

The effective porosity is calculated from:

$$\phi_e = \sqrt{\frac{(\phi_{dc}^2+\phi_{nc}^2)}{2}} \quad (3.3)$$

where ϕ_{dc} and ϕ_{nc} are shale corrected porosities for density and neutron, respectively. In the case where neutron logs are not available, the effective porosities will only be determined from density logs. In Simandoux equation, the Volume of shale (Vsh) term does not correspond fully to the original Vsh definition because of clay mineral (montmorillonite) used in his experiments was not in a fully wetted state when the mixture was made.

3.4 Indonesia Model

In 1971, Poupon and Leveaux[2] proposed an empirical model called "Indonesia formula". This equation was developed based on the typical characteristic of fresh formation waters and high degrees of shaliness that presents in many oil reservoirs in Indonesia. In this model the conductivity relationship between **R_t** and **S_w** is a result of conductivities of the clay, formation water and additional conductivity from the interaction between both of them. The empirical relationship can be written as:

$$\frac{1}{\sqrt{R_t}} = \left[\frac{V_{sh}^{1-Vsh/2}}{\sqrt{R_{sh}}} + \frac{\phi_e}{\sqrt{R_w}} \right] . S_w \tag{3.4}$$

This equation introduced an exponent of V_{sh} that is itself a function of V_{sh} to accommodate the non-linear zone of **Figure 2** in chapter one. Effective porosity calculations are also based on equation (3.3).

3.5 LSU Model

LSU model was proposed by Lau and Bassiouni[14,15,16] as a modification of previous Silva-Bassiouni model[12] by eliminating some empirically derived correction factors so that the application can be easily extended to formation temperatures other than 25°C. This model is based on the assumption that clay counter-ions behave as an equivalent sodium chloride electrolyte.

There are two equations in LSU model that should be used together: (1) conductivity model and (2) spontaneous potential model. The conductivity and spontaneous potential are given, respectively, by:

$$C_t = \frac{S_w^{\ n}}{F_e} [\, C_{eq} \, . \, n_{eq} \, . \, v_{fdl} + (1\text{-}v_{fdl}) . \, C_w] \tag{2.5}$$

$$SP = \frac{-2.R.T}{F} \int_{m2}^{m1} m_{eff} \, d\ln(m.\gamma\pm) \tag{2.37}$$

$$+ \frac{2.R.T}{F} \int_{m2}^{m1} \left[\frac{C_{eq}.n_{eq}.v_{fdl} + t_{Na}^{\ +}.(1-v_{fdl}).C_w}{C_{eq}.n_{eq}.v_{fdl} + (1-v_{fdl}).C_w} \right] d\ln(m.\gamma\pm)$$

There are four unknowns in the above equations, namely C_w, m_{eff}, S_w, and Q_v. The best method to determine C_w is by chemical analysis of formation water samples. Because this field is characterized by low salinity formation water that makes the water analysis very sensitive to contaminant, it is difficult to determine the correct $\mathbf{C_w}$ from water analysis. The low salinity can be observed from water analysis listed in Table 3.1. The analysis is from several wells in different intervals. It is possible to calculate $\mathbf{C_w}$ and $\mathbf{m_{eff}}$ simultaneously by applying the LSU model in a clean water bearing formation because $\mathbf{S_w}$ and $\mathbf{Q_v}$ values are equal to 1 and 0, respectively. By applying the $\mathbf{C_w}$ and $\mathbf{m_{eff}}$ from clean sand water analysis to LSU model in shaly sand containing potential hydrocarbon, $\mathbf{S_w}$ and $\mathbf{Q_v}$ can also be determined simultaneously. The consistency of $\mathbf{C_w}$ and $\mathbf{m_{eff}}$ calculated in water zone from several wells using LSU model can be observed in Table 3.2. This result shows that LSU model is a better tool for determining the both parameters where other methods have failed.

Table 3.1 – Water salinity analysis from different well in different intervals

Well	Formation	NaCl Eq. (ppm)
B	Z	1758.7
	Z	342.6
	Z	472.9
C	Y	2887.3
D	Z	595.7
	Z	853.8
	Z	762.3
G	Z	732.4
M	X	5556.1
	Z	143.7
N	Z	1433.5
	Z	1510.6
O	Z	650.2
P	Z	352.6
Q	Z	698.7
R	Z	930.6

Table 3.2 – Water conductivity and membrane efficiency calculated from LSU models

Well	Cw (mho-m)	meff
B	1.441	0.946
C	1.656	1.025
D	1.537	1.040
E	1.691	1.025
P	1.423	1.091
S	1.547	0.836
T	1.527	1.098
U	1.537	1.040

The input data for LSU model consist of: spontaneous potential (SP), formation conductivity (**C_t**), and formation factor (**F_e**). While SP and C_t can be determined directly from the logs, F_e need to be calculated using:

$$\mathbf{F_e} = \frac{\mathbf{a}}{\phi^{\mathbf{m}}} \tag{3.5}$$

In order to get an accurate F_e, the value of **a** and **m** usually need to be determined using special core analysis. Unfortunately, there are no core data available in Y formation, so all the evaluation are using core data from the formation above and below the zone of interest such as X and Z formation. An **a** value of 1 and **m** value of 1.6 were determined from the average value from all the cores because they all corresponded to a similar trend as shown in **Figure 3.2**. Those values will be used to determine the formation factor, F_e, for the rest of the wells.

In some of the wells porosity, ϕ, are determined using the neutron-density cross-plot method, while in most of the other wells the porosity data can be determined either from density log or neutron log alone. The porosities obtained from cross-plot or one log method was compared to porosity from core analysis of well B, well K and well L. The result showed a reasonable agreement (**Figure 3.3**).

The measured porosity and formation factor values are listed in Table 3.3.

Table 3.3 – Measured formation factor from special
special core analysis

Well	Formation	Depth	Porosity	Fe
B	Z	5122.0	0.176	16.332
		5133.1	0.161	17.177
		5136.8	0.181	15.441
		5144.8	0.373	4.615
		5151.8	0.181	15.702
		5168.5	0.207	13.011
		5184.3	0.195	13.354
		5192.2	0.211	12.444
		5212.6	0.164	17.545
K	Z	5134.9	0.183	15.064
		5154.2	0.226	10.891
		5166.5	0.197	13.308
		5183.4	0.202	12.659
		5196.0	0.138	23.535
		5204.5	0.197	13.212
L	X1	4670.5	0.209	13.529
		4686.3	0.229	10.953
		4696.5	0.253	9.793

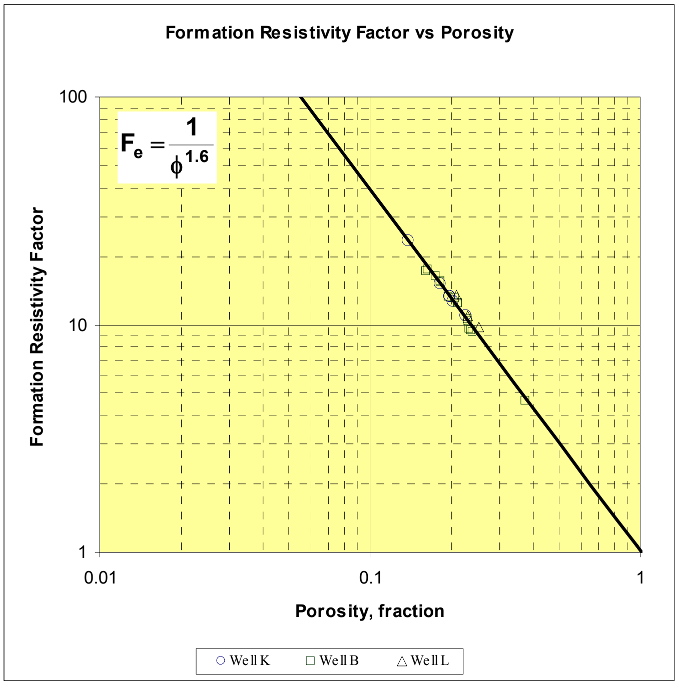

Figure 3.2 – Relationship between formation factor (F_e) and porosity (ϕ) from special core analysis

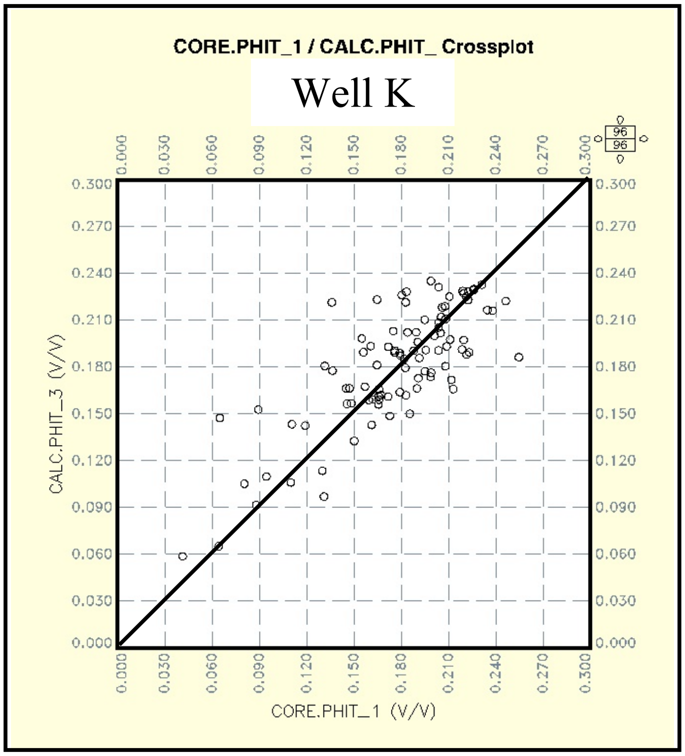

Figure 3.3 – Comparison of measured vs. calculated porosity of Z formation

3.6 Result Analysis and Discussion

Log data of Y formation from 11 wells were analyzed using various shaly sand interpretation models. These wells were chosen because of the availability of production data from the interval analyzed. The water cut (**f_w**) will be used to validate the calculated water saturation values. Validation was done by comparing the average calculated water saturation to the production test result within the same test interval.

Since Y formation in these different wells were from the same depositional environment, therefore the clay type and formation water resistivity were also presumably similar. This similarity made it possible to use some parameters that could directly be calculated using data from one well, such as water conductivity and membrane efficiency, to other near by well where direct calculation was not possible.

Archie model was used to generate a base value. It is known that in a shaly sand formation, this technique overestimated the value of water saturation. Thus, in a shaly formation, a shaly sand model should yield a saturation value less than that given by Archie's model. How much can other model results differ from Archie's in a shaly formation will be evaluated using some core and fluid analysis data.

Figure 3.4a indicated that at well C, the existing perforation intervals were set on 70% of water saturation cut off. This cut off is based on the commonly used Indonesia model.

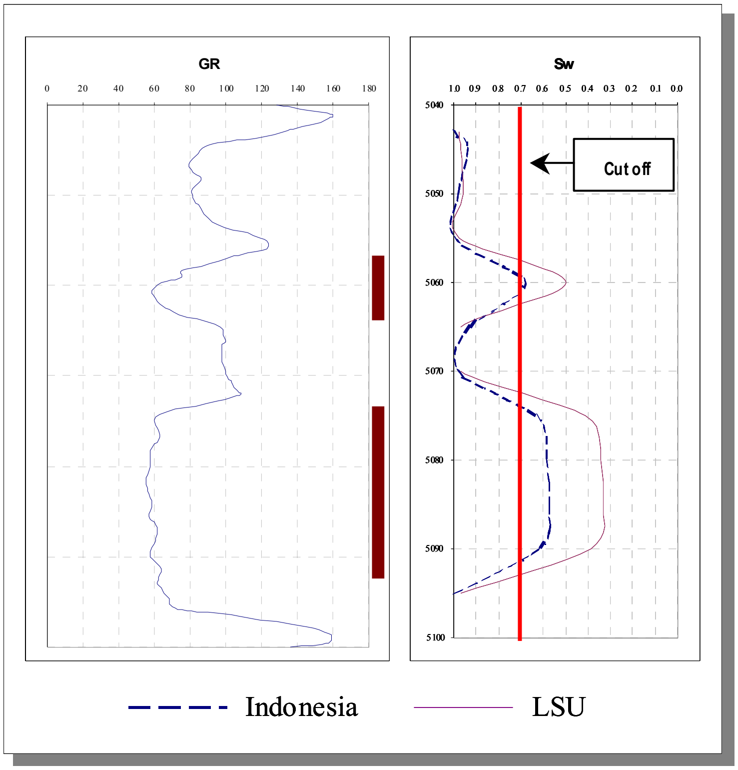

Figure 3.4a – Water saturation comparison between Indonesia and LSU models at well C

However, as shown in **Figure 3.4b** this model has failed to identify a potential hydrocarbon zone at well B in the upper part of Y formation because the calculated water saturations are above the water saturation cut off. On the other hand, in the same zone, LSU model has indicated a potential bypassed hydrocarbon potential. The validation of LSU model using production data is very important to improve the confidence of its calculation result.

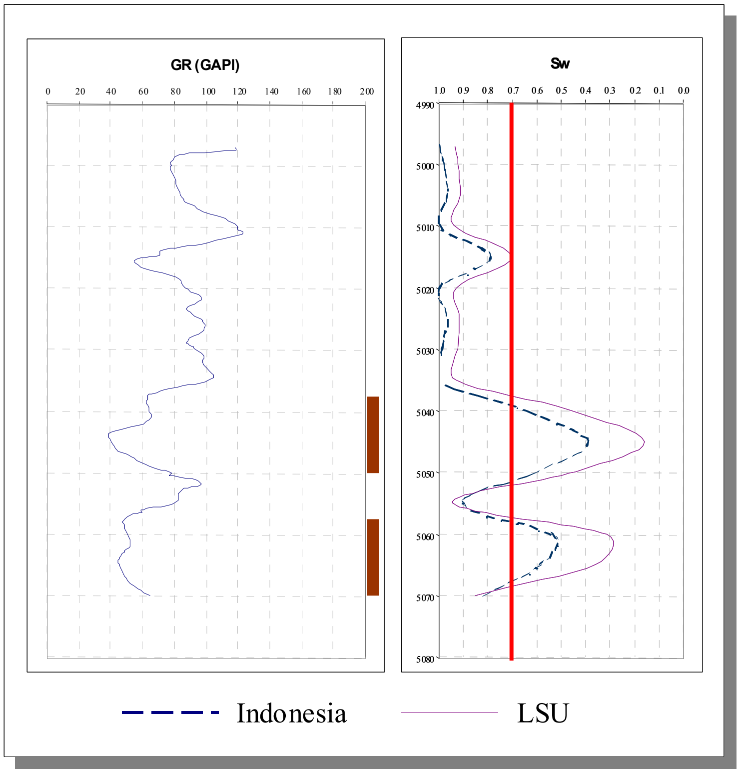

Figure 3.4b – Water saturation comparison between Indonesia and LSU models at well B

Figure 3.5 shows a comparison of the result from LSU model and the others such as Archie, Simandoux and Indonesia model from all wells. This graph clearly indicates that the water saturations calculated from LSU model are approximately 20% lower than others. In most of the cases result from Simandoux and Indonesia model are very close to the result of Archie model. Since the Archie could not generate a good estimation of water saturation in shaly sand formation, therefore Simandoux and Indonesia are not appropriate models for this formation.

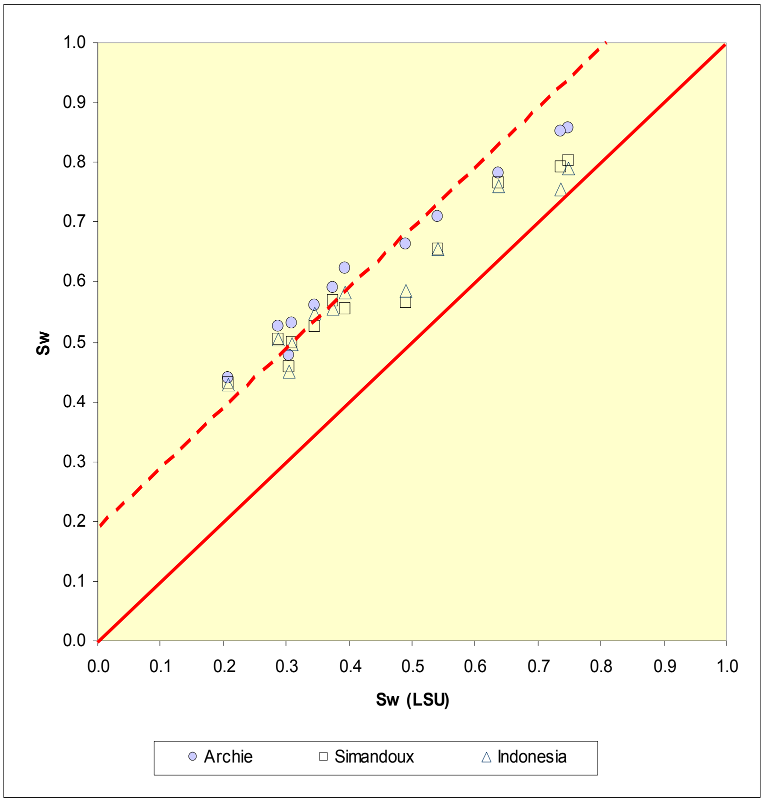

Figure 3.5 – Comparison of calculated water saturation between LSU model and Archie, Simandoux and Indonesia model from 11 wells.

The difference between Simandoux and Indonesia models from Archie's can be observed from **Figure 3.6**. Water saturation calculation from both equations showed approximately 5% - 7% lower than Archie method. In fact in the range of saturation of interest, i.e 20%-40%, these three methods give the same value. The insignificant difference made by these two methods compared to Archie method has demonstrated that Simandoux and Indonesia model are not making a substantial improvement of water saturation analysis in this particular shaly sand reservoir characterized by low water salinity formations.

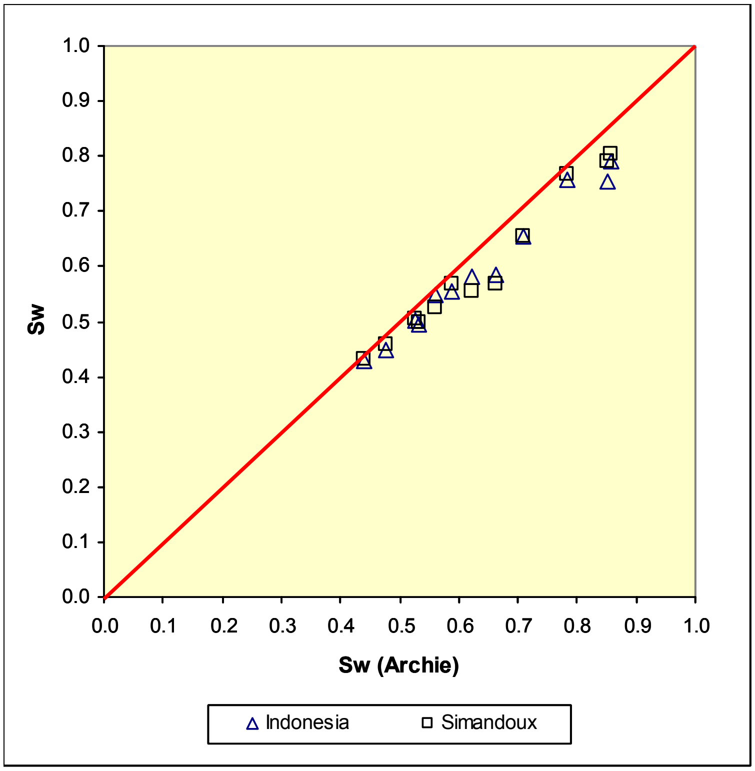

Figure 3.6 – Calculated water saturation of Simandoux and Indonesia model compare to Archie model

The relationship between calculated result and actual test data was done by comparing the average calculated water saturation within the perforated zone with the fractional water, $\mathbf{f_w}$, calculated from production test.

Figure 3.7 shown a familiar shape of the relationship between the calculated water saturation and fractional water from production data using LSU and Indonesia models. Unlike the result from Indonesia models, the irreducible water saturation, S_{wirr}, of 27% and residual oil saturation, S_{or}, of 30% from LSU correspond well to those from core analysis of several wells. Core analysis indicated value of 20% - 30% of irreducible water saturation and 30% - 40% of residual oil saturation. The other points (**Figure 3.7**) that fall off from the common trend were possibly caused by water channeling from the watered out Z formation below.

Table 3.4 – Water cut data and calculated water saturation result

Well	**Water Cut (fw),** fraction	**Water Saturation (Sw),** fraction		
		Indonesia	**Simandoux**	**LSU**
A	0.96	0.727	0.676	0.735
B	0.05	0.502	0.477	0.276
C	0.28	0.645	0.645	0.557
D	1.00	0.670	0.647	0.684
E	0.10	0.563	0.577	0.617
	0.60	0.618	0.550	0.611
F	0.99	0.742	0.745	0.638
G	0.10	0.564	0.568	0.435
H	0.20	0.558	0.572	0.443
I	0.70	0.503	0.504	0.287
J	0.98	0.452	0.448	0.236
L	0.80	0.648	0.636	0.581

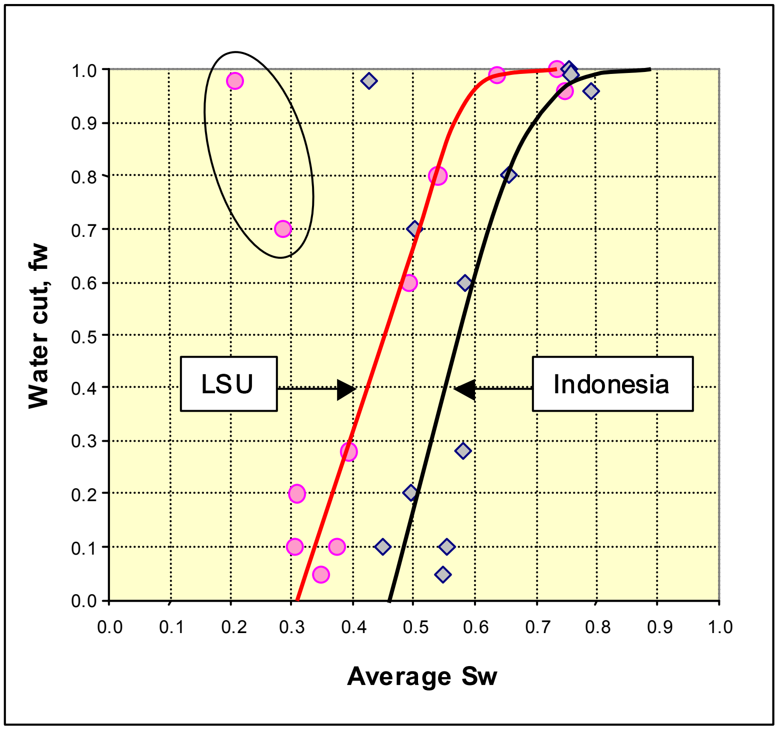

Figure 3.7 – Relationship between average calculated water saturation and fractional water value from production test using LSU and Indonesia model

CHAPTER 4

SHALY SAND INTERPRETATION ALGORITHM

The practical approach to the use of the LSU model is to set up a comprehensive spreadsheet that incorporates the conductivity and membrane potential models. This spreadsheet can then be used for all the simultaneous calculations.

Preparation and quality check of all input data is very important to a representative output, especially for low SP deflection, which is encountered in low - salinity of the formation water conditions. Simple statistical methods can be used to determine the data distribution and to make a reasonable normalization. Borehole corrections are applied to resistivity and neutron-density data to determine the input conductivity and porosity, respectively.

There are typically four keys unknown parameters that need to be determined using both the conductivity and the membrane potential model. The four parameters are water conductivity (**C_w**), membrane efficiency (**m_{eff}**), cation exchange capacity (**Q_v**), and water saturation (**S_w**). It is necessary to assign a temporary value for the unknown in order to set up the calculation spreadsheet. The average value of water conductivity determined from laboratory analysis is a good starting point for C_w. Local knowledge of membrane efficiency is a valuable source a preliminary assigned value for m_{eff}; Value between 0.8 to 1.0 are also applicable. S_w value of 1 and Q_v value of 0 are also a reasonable preliminary value for establishing the comprehensive spreadsheet.

The algorithm described hereafter is a step-by-step approach using a set of data from one depth point. Same steps are repeated for the rest of intervals of interest.

4.1 The Algorithm of Conductivity Model

The conductivity model analysis is based on the following equation:

$$\mathbf{C_t = \frac{S_w{}^n}{F_e}[\,C_{eq}\,.\,n_{eq}\,.\,v_{fdl} + (1\text{-}v_{fdl}).\,C_w]} \qquad (2.5)$$

The calculation algorithm of LSU conductivity model to interpret the water saturation in a shaly sand is shown in **Figure 4.1** and described as following:

1. Prepare the temperature data in two units: $\mathbf{T_a}$ in Kelvin and **T** in Celcius.
2. Calculate the molarity of sodium chloride solutions ($\mathbf{n_1}$) and mud filtrate ($\mathbf{n_2}$), using a preliminary assigned value of $\mathbf{C_w}$ and the value of $\mathbf{C_{mf}}$ from mud data:

$$\mathbf{\ln(n_1) = 68.1 - 13.5791\ \ln(T_a) + 2.289\text{x}10^{-2} + 1.1854\ \ln(C_w) + 4.6761\text{x}10^{-3}\ C_w} \qquad (2.30)$$

$$\mathbf{\ln(n_2) = 68.1 - 13.5791\ \ln(T_a) + 2.289\text{x}10^{-2} + 1.1854\ \ln(C_{mf}) + 4.6761\text{x}10^{-3}\ C_{mf}}$$

3. Calculate the double layer thickness, $\mathbf{f_{dl}}$:

$$f_{dl} = \mathbf{\sqrt{T_a\,/\,6.18^2.Bo^2.n_1.298}} \qquad (2.28)$$

where:

$$\mathbf{B_o = 0.3248 + 1.5108\ x\ 10^{-4}\ T + 8.935\text{x}10^{-7}\ T^2} \qquad (2.29)$$

4. Calculate fractional volume of double layer, $\mathbf{v_{fdl}}$, using a preliminary assigned value of cation exchange capacity, $\mathbf{Q_v}$:

$$\mathbf{v_{fdl} = (0.28 - 0.0344\ \ln(T/25))\ .\ f_{dl}\ .\ Q_v} \qquad (2.27)$$

5. Calculate the equivalent counter-ion concentration, $\mathbf{n_{eq}}$:

$$\mathbf{n_{eq}} = \frac{\mathbf{Q_v}}{\mathbf{v_{fdl}}} \cdot \frac{\mathbf{T_a}}{\mathbf{298}} \tag{2.25}$$

6. Calculate the molar counter-ion conductivity, $\mathbf{c_{eq}}$:

$$\mathbf{c_{eq}} = \mathbf{exp}\,(-\mathbf{58.84} - \mathbf{0.1026}\,\mathbf{n_{eq}} - \mathbf{0.0787}\,\mathbf{ln(n_{eq})} - \mathbf{0.0216}\,\mathbf{T_a} + \mathbf{11.85}\,\mathbf{ln}\,\mathbf{T_a} \tag{2.26}$$

7. Calculate the true conductivity, $\mathbf{C_t}$ by using a preliminary assigned $\mathbf{S_w}$:

$$\mathbf{C_t} = \frac{\mathbf{S_w}^{\mathbf{n}}}{\mathbf{F_e}}\left[\mathbf{c_{eq}} \cdot \mathbf{n_{eq}} \cdot \mathbf{v_{fdl}} + (\mathbf{1} - \mathbf{v_{fdl}}) \cdot \mathbf{C_w}\right] \tag{1.7}$$

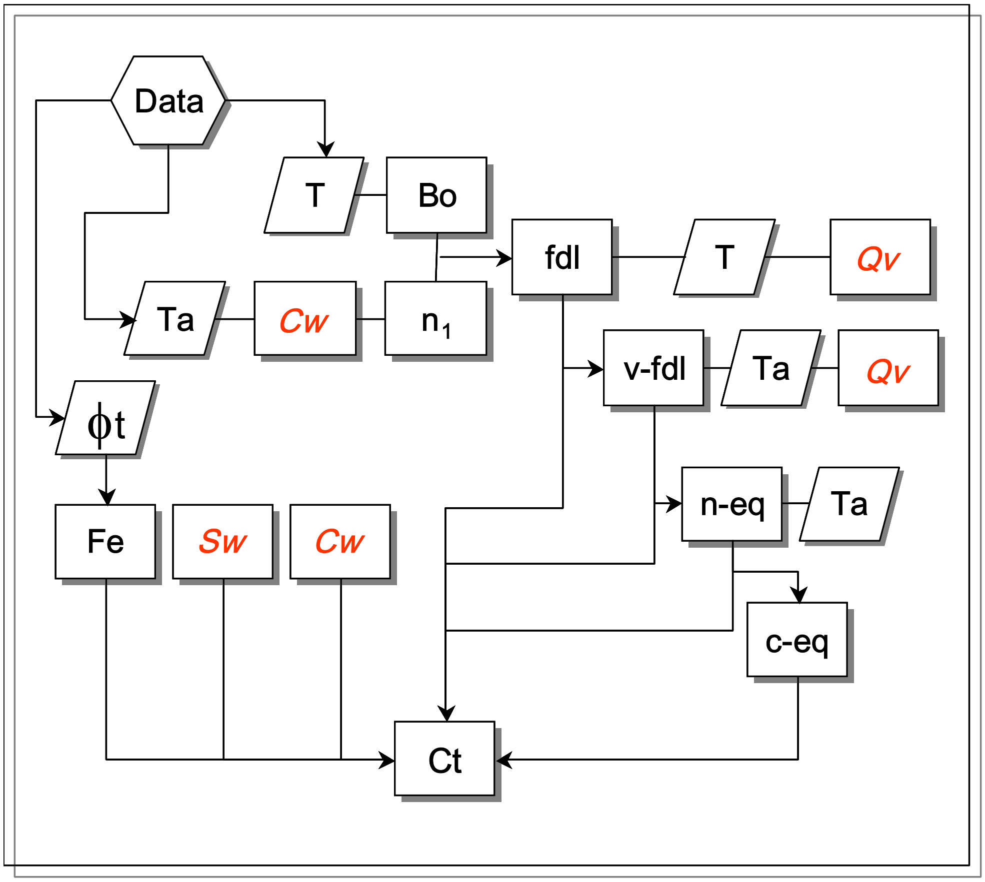

Figure 4.1 – Flow chart of formation conductivity calculation using Conductivity Model

4.2 The Algorithm of Membrane Potential Model

The analysis of Membrane Potential model is based on the following equation:

$$\mathbf{SP} = \frac{-2.R.T}{F}\int_{m2}^{m1} m_{eff}\, d\ln(m.\gamma\pm) \tag{2.37}$$

$$+\frac{2.R.T}{F}\int_{m2}^{m1}\left[\frac{C_{eq}.n_{eq}.v_{fdl}+t_{Na}{}^{+}.(1-v_{fdl}).C_{w}}{C_{eq}.n_{eq}.v_{fdl}+(1-v_{fdl}).C_{w}}\right] d\ln(m.\gamma\pm)$$

The equation consists of two parts: first part is known as sodium transport number in shale and second part is in sandstones. In order to calculate spontaneous potential (SP), the equation above will be evaluated in two separate calculations then combined together at the end. Both calculations can be done using a simple trapezoid rule. Equation 2.37 will be schematically expressed as:

$$\mathbf{SP} = \frac{-2.R.T}{F}\,(m_{eff}{}^{+} + h.T_{Na}{}^{+}) \tag{4.1}$$

4.2.1 Determination of $m_{eff}{}^{+}$:

Figure 4.2 shows the algorithm to calculate $\mathbf{m_{eff}{}^{+}}$, with each step describe as following:

1. Calculate the molality of sodium chloride solutions ($\mathbf{m_1}$) and mud filtrate ($\mathbf{m_2}$):

$$\ln(m_1) = 1.5054 + 1.0142\ln(n_1) + 0.2721\ln(T_a) \tag{2.45}$$

$$\ln(m_2) = 1.5054 + 1.0142\ln(n_2) + 0.2721\ln(T_a)$$

2. Calculate the mean activity coefficient, $\gamma\pm$:

$$\log(\gamma\pm)^a = \log(\gamma\pm^{298})^a + 0.5Y\,.\,L_{298}{}^{a} - 0.5Z.\,J_{298}{}^{a} \tag{2.40}$$

$$\log(\gamma\pm)^b = \log(\gamma\pm^{298})^b + 0.5Y.\,L_{298}{}^{b} - 0.5Z.\,J_{298}{}^{b}$$

where:

$$\log\,(\gamma\pm^{298})^a = \frac{-0.5115\sqrt{n_1}}{1+1.3065\sqrt{n_1}} - 1.75\log(a_A)^a - \log(1-0.027\,m_1) \quad (2.23)$$

$$\log\,(\gamma\pm^{298})^b = \frac{-0.5115\sqrt{n_2}}{1+1.3065\sqrt{n_2}} - 1.75\log(a_A)^b - \log(1-0.027\,m_2)$$

$$(a_A)^a = 0.99948 - 3.0959\text{x}10^{-2}\,(m_1) - 0.0015\,m_1^2 \quad (2.24)$$

$$(a_A)^b = 0.99948 - 3.0959\text{x}10^{-2}\,(m_2) - 0.0015\,m_2^2$$

$$Y = \frac{298.15 - T_a}{8.3147\,(298.15)\,2.3026\,(T_a)} \quad (2.41)$$

$$Z = 298.15\ Y + \frac{1}{8.3147}\log(T_a\,/\,298.15) \quad (2.42)$$

$$L_{298}{}^a = \frac{2878.6\sqrt{m_1}}{1+\sqrt{m_1}} - 3182.8\,m_1 + 986.5\sqrt{m_1{}^3} \quad (2.43)$$

$$L_{298}{}^b = \frac{2878.6\sqrt{m_2}}{1+\sqrt{m_2}} - 3182.8\,m_2 + 986.5\sqrt{m_2{}^3}$$

$$J_{298}{}^a = \frac{43.5\sqrt{m_1}}{1+\sqrt{m_1}} + 72\,m_1 - 20.36\sqrt{m_1{}^3} \quad (2.44)$$

$$J_{298}{}^b = \frac{43.5\sqrt{m_2}}{1+\sqrt{m_2}} + 72\,m_2 - 20.36\sqrt{m_2{}^3}$$

3. Solving the first part of the equation calculate $\mathbf{m_{eff}}^+$, using a temporary assigned $\mathbf{m_{eff}}$:

$$m_{eff}{}^+ = m_{eff}\,(\ln(m_1.\,\gamma\pm^a) - \ln(m_2\,.\,\gamma\pm^b)) \quad (4.2)$$

$m_{eff}{}^+$ is equal to $\int_{m2}^{m1} m_{eff}\,d\ln(m.\gamma\pm)$

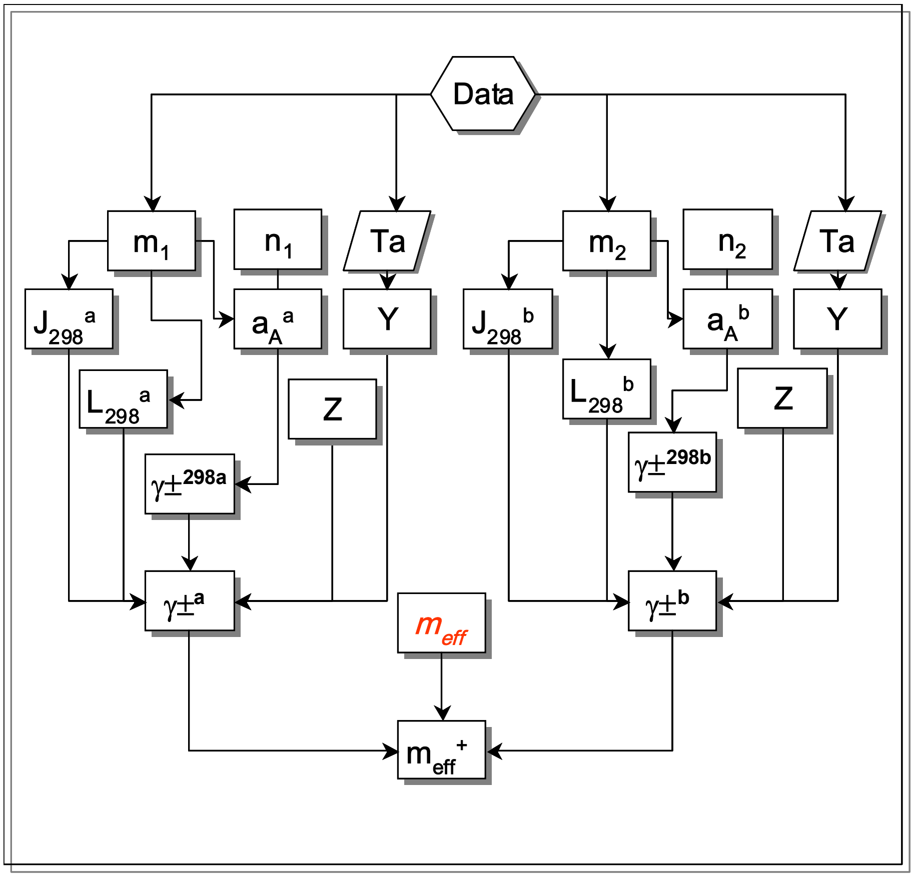

Figure 4.2 – Flow chart of $\mathbf{m_{eff}^{+}}$ calculation using Membrane Potential Model

4.2.2 Determination of T_{Na}^{+}:

Figure 4.3 shows the algorithm to calculate T_{Na}^{+}, with detail description as following:

1. Divided the differences between $\mathbf{m_1}$ and $\mathbf{m_2}$ by 100:

$$\mathbf{h = \frac{m_1 - m_2}{100}} \tag{4.3}$$

2. Set up a spreadsheet started with $\mathbf{m_2}$ and keep adding h until it reach the value of $\mathbf{m_1}$.

3. For every point on step no.2, calculate hittroff transport number, $\mathbf{t_{Na}^{ht}}$:

$$\mathbf{\ln(t_{Na}^{ht}) = -2.5089 - 1.8038x10^{-2} \ln(m_1) + 0.2647 \ln(T_a) - 1.4176x10^{-5}\, T_a.m_1} \qquad (2.47)$$

4. For every point on step no.2, calculate the water transport number, $\mathbf{t_w}$:

$$\mathbf{t_w = 0.053\, m_1 - 0.43 + (0.1961 \ln(m_1) + 0.1244).Q_v\ ;} \text{ for } m \leq 1.0 \qquad (2.48)$$

$$\mathbf{t_w = 0.036\, m_{11.1} - 0.04377 + 0.04.Q_v\ ;} \qquad \text{for } m > 1.0 \qquad (2.49)$$

5. For every point on step no.2, calculate the sodium chloride transport number, $\mathbf{t_{Na}^+}$ with equation:

$$\mathbf{t_{Na}^+ = t_{Na}^{ht} + t_w} \qquad (2.46)$$

6. For every point on step no.2, calculate the $\mathbf{T_{Na}^+}(i)$:

$$\mathbf{T_{Na}^+}(i) = \frac{\mathbf{c_{eq}.n_{eq}.v_{fdl} + t_{Na}^{+}(1 - v_{fdl}).C_w}}{\mathbf{c_{eq}.n_{eq}.v_{fdl} + (1 - v_{fdl}).C_w}} \qquad (2.19)$$

7. Calculate $\mathbf{T_{Na}^+}$ by adding together all the $\mathbf{T_{Na}^+}(i)$:

$$\mathbf{T_{Na}^+ = (}\ 0.5\mathbf{T_{Na}^+}(1) + \mathbf{T_{Na}^+}(2) + \ldots. + 0.5\ \mathbf{T_{Na}^+}(101)\ \mathbf{)} \qquad (4.4)$$

8. Solving the second part of the equation by multiplying **h** and $\mathbf{T_{Na}^+}$.

$\mathbf{h.T_{Na}^+}$ is equal to $\displaystyle\int_{m2}^{m1} \left[\frac{\mathbf{C_{eq}.n_{eq}.v_{fdl} + t_{Na}^{+}.(1 - v_{fdl}).C_w}}{\mathbf{C_{eq}.n_{eq}.v_{fdl} + (1 - v_{fdl}).C_w}} \right] \mathbf{d\ln(m.\gamma\pm)}$

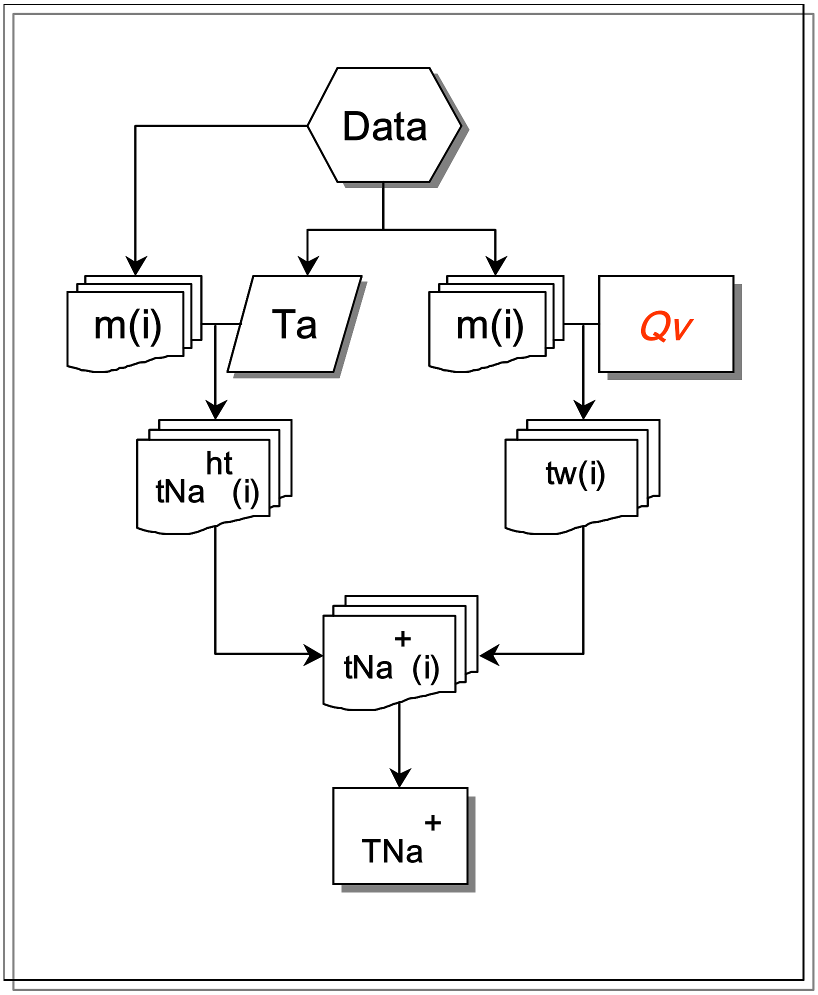

Figure 4.3 – Flow chart of TNa^+ calculation using Membrane Potential Model

4.3 The Simultaneous Solution

The calculated data that has been arranged in a spreadsheet format, are used as a pre-set up data with four keys unknown namely C_w, M_{eff}, Q_v, and S_w. The real calculations should commence when the measured input data from the log such as spontaneous potential (**SP**) and the formation conductivity (**C_t**) are incorporated.

In a water-bearing clean sand formation, two key parameters are known. They are the water saturation, **S_w**, equal to 1 and the cation exchange capacity, **Q_v**, equal to 0. Therefore the other two unknown namely water conductivity (**C_w**) and membrane efficiency (**m_{eff}**) can be calculated simultaneously.

To evaluate water-bearing shaly sand, there are three keys unknown: water conductivity (C_w), water saturation (S_w), and cation exchange capacity (Q_v). Using an iteration approach, these unknown can also be determined.

In hydrocarbon-bearing shaly sand, LSU models provide a possibility to calculate water saturation (S_w) and the cation exchange capacity (Q_v) simultaneously by incorporating the previous information found either in water-bearing clean sand formation or shaly sand.

CHAPTER 5

CONCLUSIONS

Modified Silva-Bassiouni model known as LSU models are based on cation exchange capacity and dual water concept where it treats the excess conductivity generated by the counter-ions associated with clay bound water as that of an equivalent sodium chloride solution. The models make use of a conductivity and a spontaneous potential model.

Using log data from 11 well of JR field in Central Sumatra Basin,Indonesia, these models were a superior to Vsh models in predicting the hydrocarbon potential of shaly sands containing low-salinity formation water. This is because of its ability to take into account not only the amount of shale in the formation but also the clay type. The analysis of irreducible water saturation and residual oil saturation using water cut data from production tests and special core analysis are in good agreement with the calculated water saturation using LSU models.

In clean water-bearing sand, water conductivity, C_w, and the membrane efficiency, $m_{eff,}$ can be solved simultaneously. The results were more consistent and showed a better estimation of C_w compared to other conventional methods. The ability of LSU models to determine the cation exchange capacity, Q_v, from log data has created an opportunity to supplement the Q_v data which usually obtained from conventional core analysis.

NOMENCLATURE

a = Archie's constant

a_A = equivalent ion size, Å

B = Waxman's equivalent counter-ion conductivity

C_{cl} = clay conductivity, mho-m

C_{eq} = equivalent counter-ion conductivity, mho-m

C_{eq}' = equivalent vounter-ion conductivity for $S_w < 1$, mho-m

C_{mf} = mud filtrate conductivity, mho-m

C_{sh} = shale conductivity, mho-m

C_o = conductivity of formation fully saturated with water, mho-m

C_t = formation conductivity, mho-m

C_w = water conductivity, mho-m

C_{we} = equivalent water conductivity, mho-m

CwN = water conductivity at the neutral point, mho-m

Em = electrochemical potential, mV

Em_{sh} = electrochemical potential across shales, mV

Em_{ss} = electrochemical potential across shaly sand, mV

F = Faraday's constant

F = formation factor

F* = formation factor in W-S model

F_e = formation factor in LSU model

F_o = formation factor in D-W model

f_{dl} = expansion factor of the double layer

f_g = empirical correction factor

$F_{(ne)}$ = empirical correction factor

GR = gamma ray log reading, API

J = total current in system

J_{Na}^{c} = current carried by clay counter-ion

J_{Na}^{b} = current carried by Na+ ions in the bulk phase

m = molality, mol/Kg H_2O

m = cementation exponent

m_{eff} = membrane efficiency

n = molarity, mol/l

n = saturation exponent

n_{eq} = equivalent counter-ion concentration, mol/l

Q_v = cation exchange capacity, meq/cc

Q_v’ = cation exchange capacity for $S_w < 1$, meq/cc

R = universal gas constant

R_{sh} = shale resistivity, ohm/m

R_t = formation resistivity, ohm/m

R_w = formation water resistivity, ohm/m

SP = spontaneous potential log reading, mV

S_w = water saturation, fraction

T = temperature, ^oC

Ta = absolute temperature, ^oK

T_{Na}^{+} = sodium transport number

t_{Na}^{hf} = Hittorf transport number

T_{Na}^{sh} = shale transport number

T_{Na}^{ss} = shaly sand transport number

t_{fw} = free water transport number

t_{w} = water transport number

v_{fdl} = fractional volume of the double layer

v_{fdl}' = fractional volume of the double layer for $S_w < 1$

V_{sh} = fractional volume of shale, fraction

X_H = 6.18 Å

α = clavier's double layer expansion factor

β = 2.05, constant

$\gamma\pm$ = mean activity coefficient

$\gamma\pm^{298}$ = mean activity coefficient at $25^{o}C$

η = empirical function of α

τ = empirical correction factor

ϕ = porosity, fraction

ϕ_{dc} = corrected density porosity, fraction

ϕ_{e} = effective porosity, fraction

ϕ_{nc} = corrected neutron porosity, fraction

ϕ_{T} = total porosity, fraction

BIBLIOGRAPHY

1. Worthington, P., “The Evolution of Shaly-sand Concepts in Reservoir Evaluation,” The Log Analyst, Jan-Feb. 1985, pp.23-40.

2. Poupon, A. and Leveaux, J., “Evaluation of Water Saturation in Shaly Formations,” Trans. SPWLA 12th Annual Logging Symposium, 1971, pp.1-2.

3. Worthington, P.F. and Johnston, P.W., “Quantitative Evaluation of Hydrocarbon Saturation in Shaly Freshwater Reservoir,” The Log Analyst, v.32, no.4, 1991, pp.356-368.

4. Archie, G.E., “The Electrical Resistivity Log as An Aid in Determining Some Reservoir Characteristics,” Trans. AIME 146, 1942, pp. 54-62.

5. Schlumberger, “Log Interpretation Principles/Application,” 1987, New York

6. Simandoux, P., “Dielectric Measurements in Porous Media and Application to Shaly Formation,” Revue del’Institut Francais du Petrole, Supplementary Issue, 1963, pp.193-215. (Translated text in SPWLA Reprint Volume Shaly Sand, July 1982)

7. Waxman M.H. and Smits, L. J., “ Electrical Conductivities in Oil-Bearing Shaly-Sands,” J.P.T., June 1968, pp. 107-122.

8. Clavier, C., Coates, G., and Dumanoir, J., “Theoretical and Experimental Bases for the Dual Water Model For The Interpretation of Shaly Sands,” SPEJ April 1984.

9. Silva, P. and Bassiouni, Z., “A Shaly Sand Conductivity Model Based on Variable Equivalent Counter-Ion Conductivity and Dual Water Concepts,” SPWLA Trans., paper RR, 1985.

10. Juhasz, I., et al., “The Central Role of Qv and Formation Water Salinity in the Evaluation of Shaly Formations,” SPWLA Trans., paper AA, 1979.

11. Silva, P., “Development of a New Conductivity Model for Shaly Sand Interpretation,” Ph.D. Dissertation, LSU, 1986, pp 117-8.

12. Silva, P. and Bassiouni, Z., “Prediction of Membrane Potentials in Shales and Shaly Sands Using the S-B Conductivity Model,” The Log Analyst, March-April 1987, pp. 129-137.

13. Smits L. J. M., "SP Log Interpretation in Shaly Sands", J.P.T., June 1968, pp. 123-136.

14. Thomas E.C.,"The Determination of Qv from Membrane Potential Measurements in Shaly Sand," Journal Pet. Tech., Sept 1976.

15. Robinson, R.A.and Stokes, H., "Electrolyte Solutions", 2nd Ed., Butterworths Scientific Publications, London, 1959.

16. Lau, M.N. and Bassiouni, Z., "Development and Field Applications of Shaly Sand Petrophysical Models Part I: The Conductivity Model", SPE Publications, SPE 20386, 1990.

17. Lau, M.N. and Bassiouni, Z., "Development and Field Applications of Shaly Sand Petrophysical Models Part II: The Spontaneous Potential Model", SPE Publications, SPE 20387, 1990.

18. Lau M.N. and Bassiouni, Z, "Development and Field Applications of Shaly Sand Petrophysical Models Part III: Field Applications", SPE Publications, SPE 20388, 1990.

19. Silva, P.L. and Bassiouni, Z.,"One Step Chart for SP Log Interpretation", CWLS Trans., Paper Q, 1985.

APPENDIX A

COMPARISON OF CALCULATED VS. EXPERIMENTAL CORE POROSITY

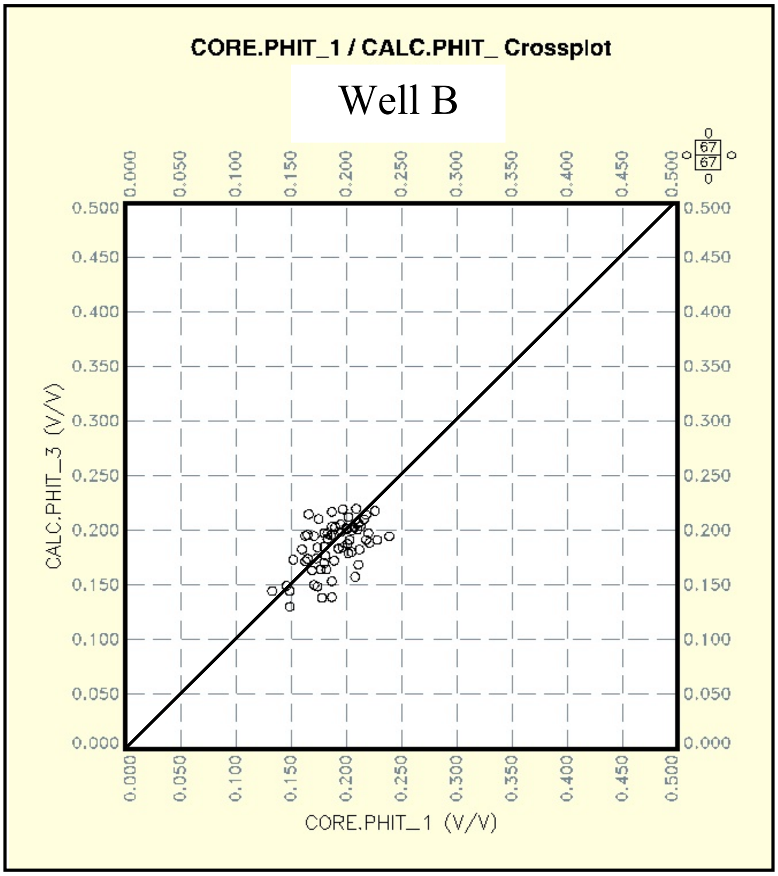
CORE.PHIT_1 / CALC.PHIT_ Crossplot
Well B
0
67
67
0
0.000
0.050
0.100
0.150
0.200
0.250
0.300
0.350
0.400
0.450
0.500
CALC.PHIT_3 (V/V)
CORE.PHIT_1 (V/V)

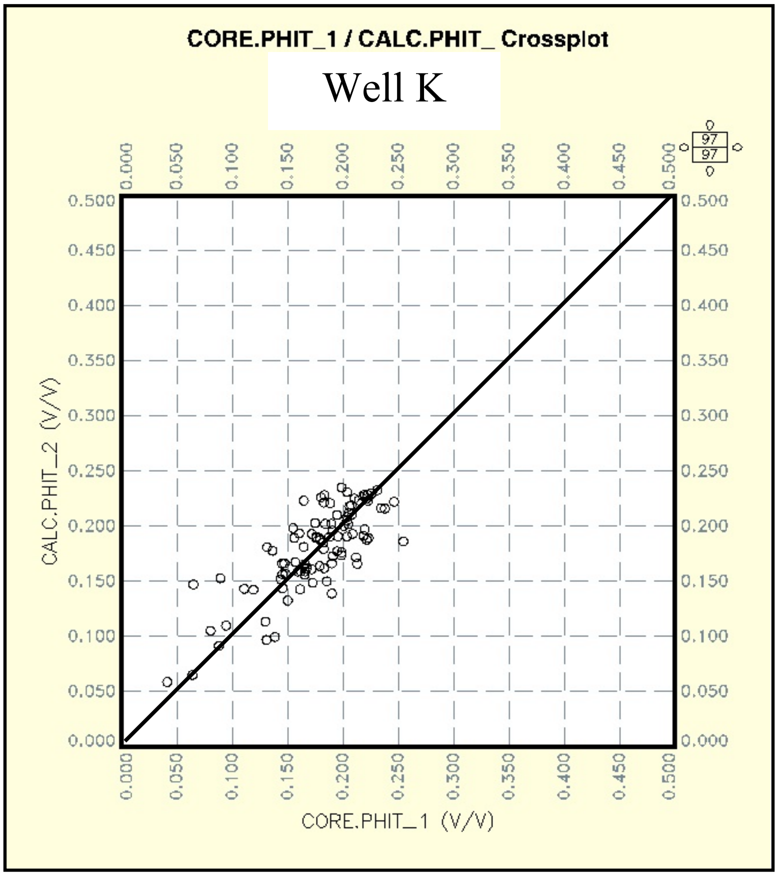
CORE.PHIT_1 / CALC.PHIT_ Crossplot
Well K
97
97
CALC.PHIT_2 (V/V)
CORE.PHIT_1 (V/V)
0.000
0.050
0.100
0.150
0.200
0.250
0.300
0.350
0.400
0.450
0.500

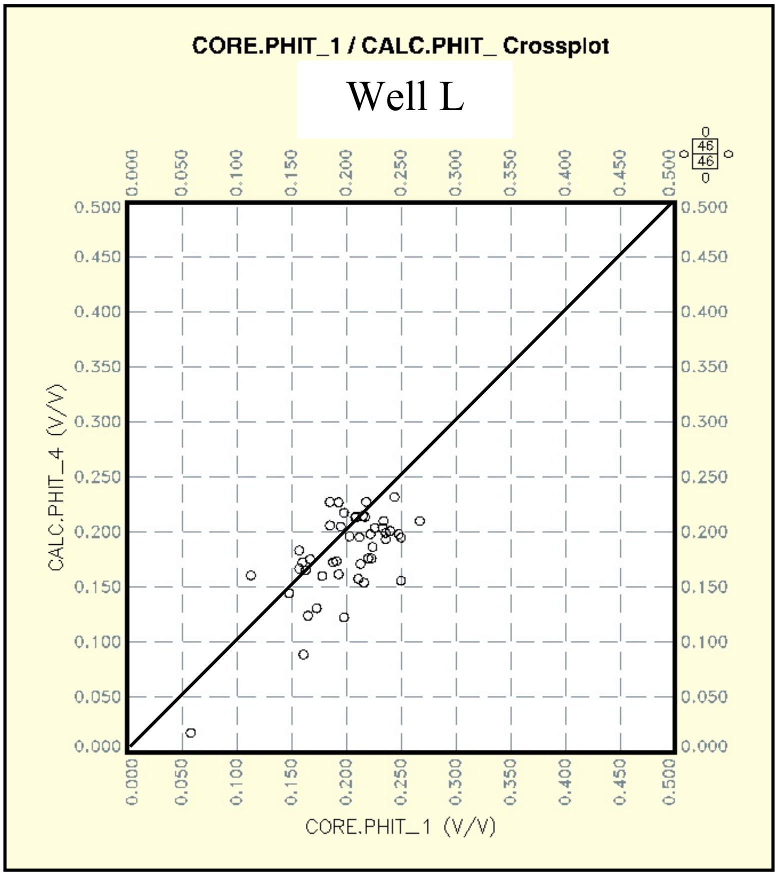
CORE.PHIT_1 / CALC.PHIT_ Crossplot
Well L
CALC.PHIT_4 (V/V)
CORE.PHIT_1 (V/V)
0.000
0.050
0.100
0.150
0.200
0.250
0.300
0.350
0.400
0.450
0.500
0
46
46
0

APPENDIX B

RESULT COMPARISON OF LSU MODEL VS. ARCHIE MODEL, SIMANDOUX MODEL AND INDONESIA MODEL

Well A

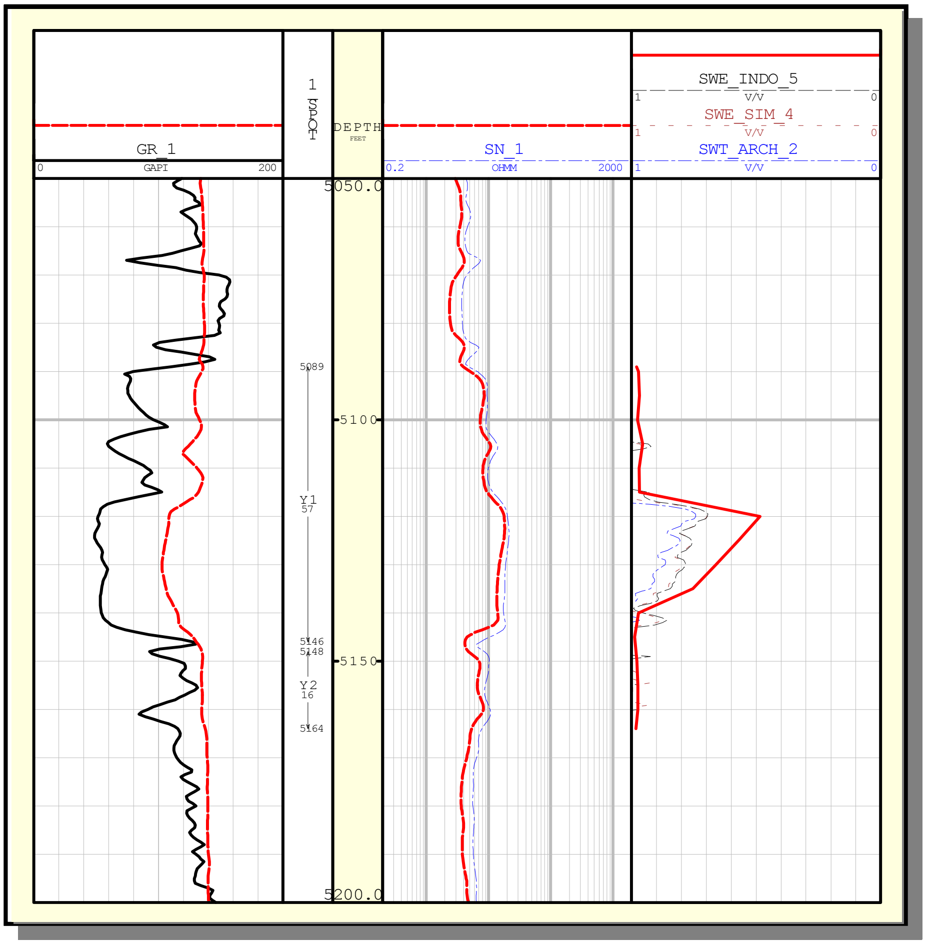
GR_1
0
GAPI
200
1
TOPS
DEPTH
FEET
SN_1
0.2
OHMM
2000
SWE_INDO_5
1
V/V
0
SWE_SIM_4
1
V/V
0
SWT_ARCH_2
1
V/V
0
5050.0
5100
5150
5200.0
5089
Y1
57
5146
5148
Y2
16
5164

Well B

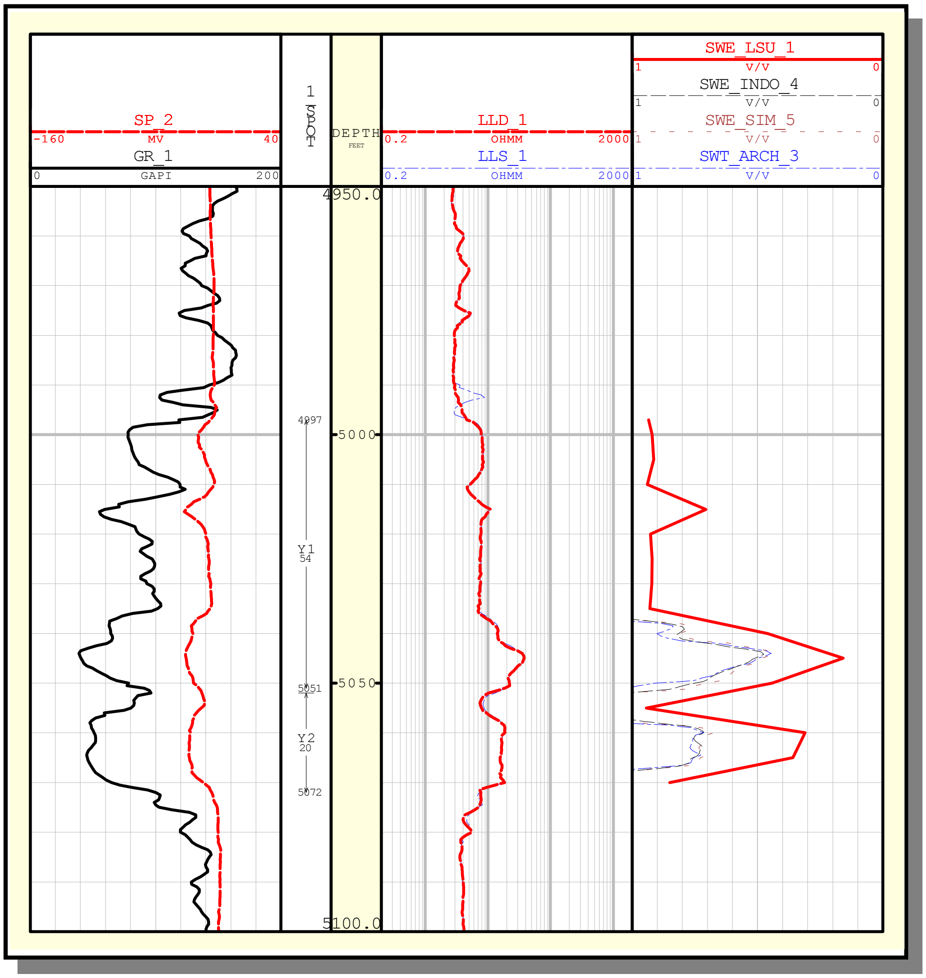

SP_2
-160
MV
40
GR_1
0
GAPI
200
TOPS_1
DEPTH
FEET
LLD_1
0.2
OHMM
2000
LLS_1
0.2
OHMM
2000
SWE_LSU_1
1
V/V
0
SWE_INDO_4
1
V/V
0
SWE_SIM_5
1
V/V
0
SWT_ARCH_3
1
V/V
0
4950.0
4997
5000
Y1
54
5050
5051
Y2
20
5072
5100.0

Well C

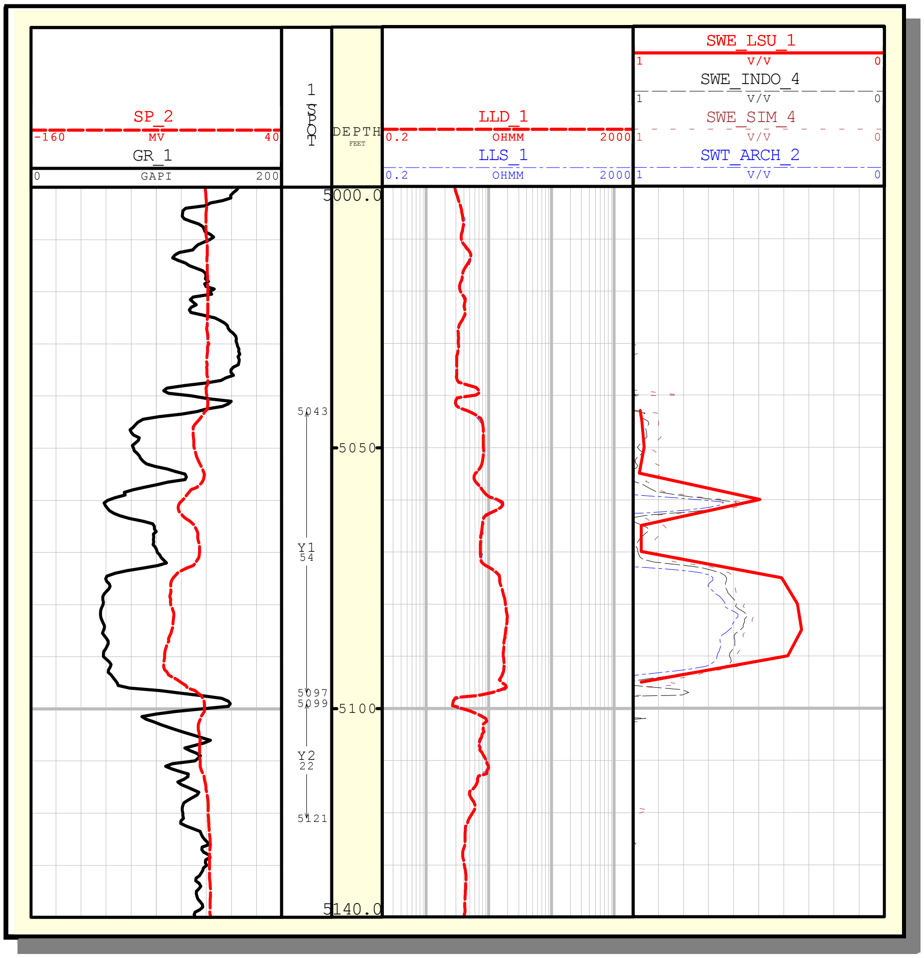

SP_2
-160
MV
40
GR_1
0
GAPI
200
1
SPOT
DEPTH
FEET
LLD_1
0.2
OHMM
2000
LLS_1
0.2
OHMM
2000
SWE_LSU_1
1
V/V
0
SWE_INDO_4
1
V/V
0
SWE_SIM_4
1
V/V
0
SWT_ARCH_2
1
V/V
0
5000.0
5043
5050
Y1
54
5097
5099
5100
Y2
22
5121
5140.0

Well D

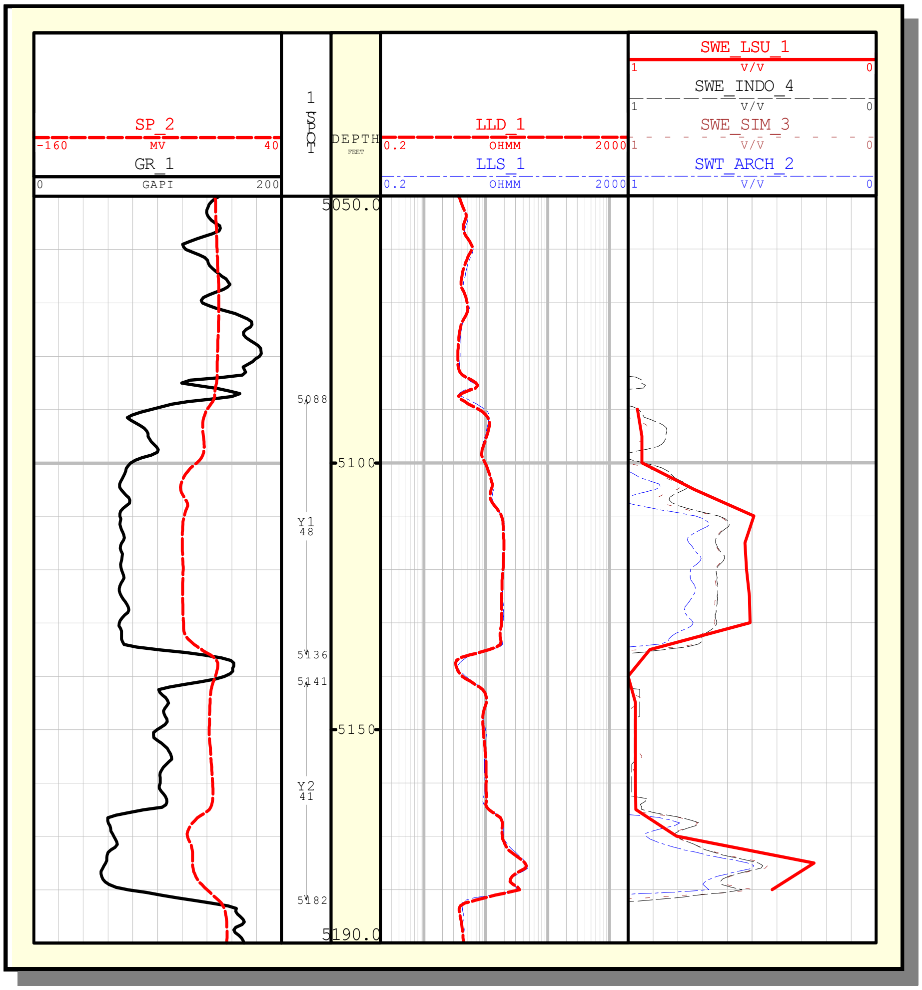

SP_2
-160
MV
40
GR_1
0
GAPI
200
1
ZONE
DEPTH
FEET
5050.0
5088
5100
Y1
48
5136
5141
5150
Y2
41
5182
5190.0
LLD_1
0.2
OHMM
2000
LLS_1
0.2
OHMM
2000
SWE_LSU_1
1
V/V
0
SWE_INDO_4
1
V/V
0
SWE_SIM_3
1
V/V
0
SWT_ARCH_2
1
V/V
0

Well E

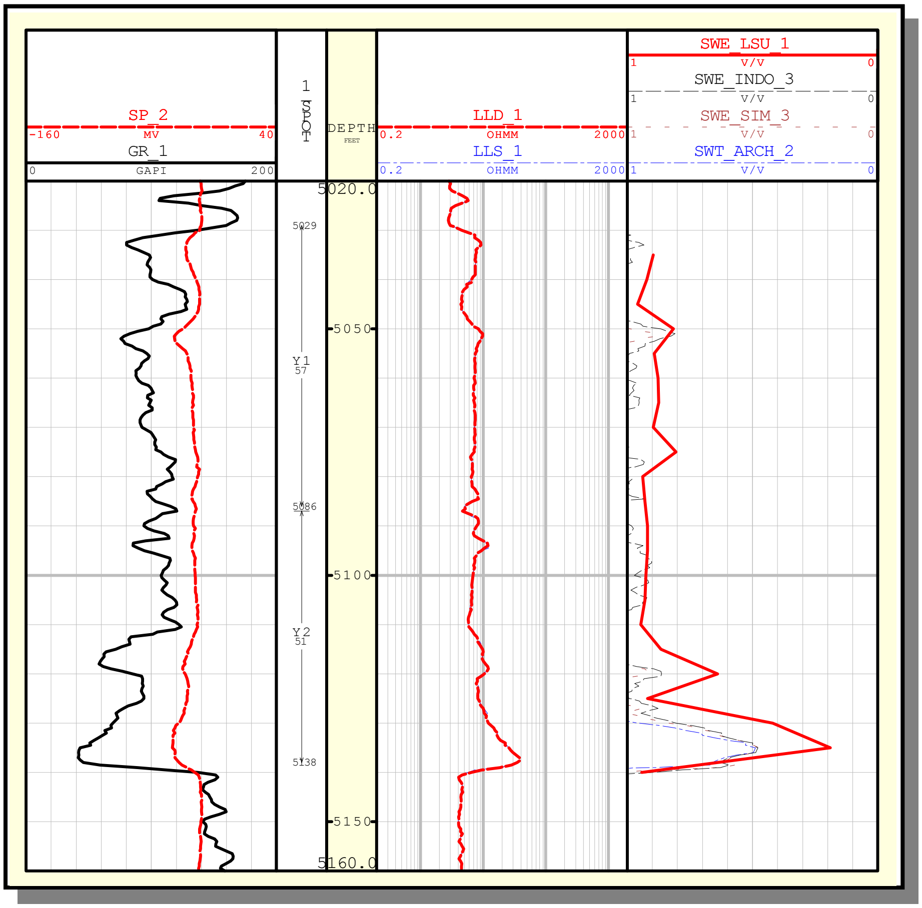
SP_2
MV
-160
40
GR_1
GAPI
0
200
DEPTH
FEET
LLD_1
OHMM
0.2
2000
LLS_1
OHMM
0.2
2000
SWE_LSU_1
V/V
1
0
SWE_INDO_3
V/V
1
0
SWE_SIM_3
V/V
1
0
SWT_ARCH_2
V/V
1
0
5020.0
5029
5050
Y1
57
5086
5100
Y2
51
5138
5150
5160.0

Well F

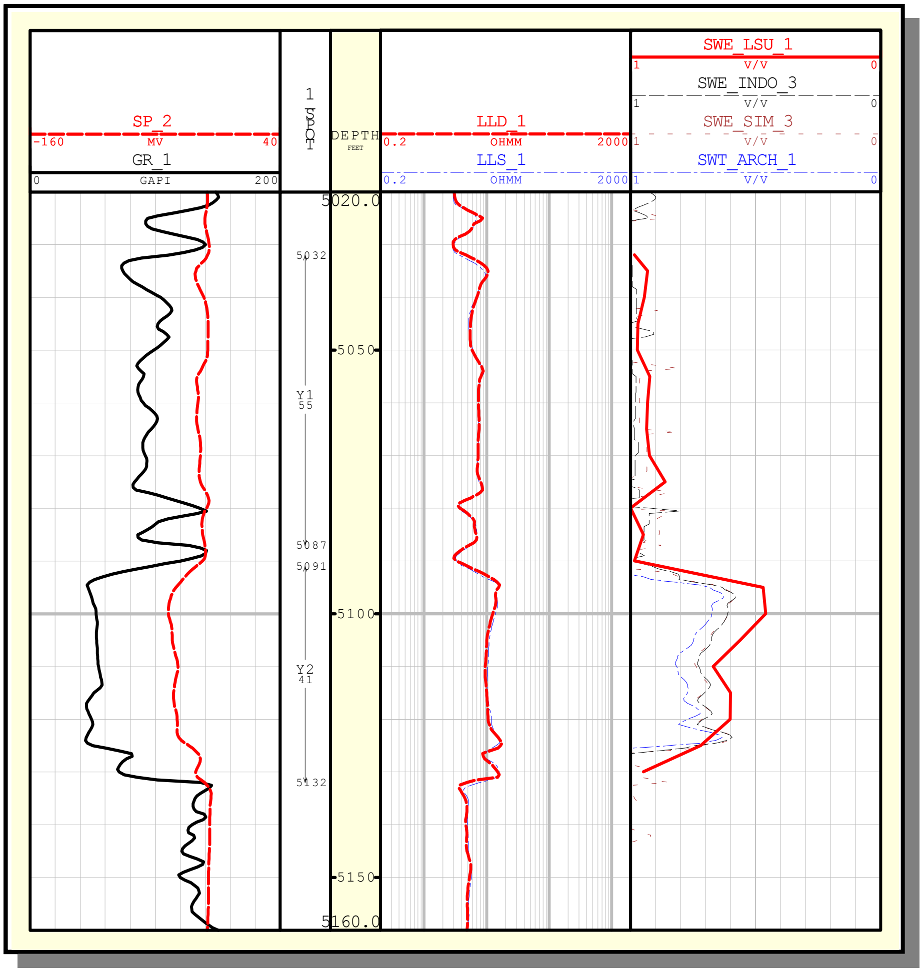
SP_2
-160
MV
40
GR_1
0
GAPI
200
1
DEPTH
FEET
5020.0
5032
5050
Y1
55
5087
5091
5100
Y2
41
5132
5150
5160.0
LLD_1
0.2
OHMM
2000
LLS_1
0.2
OHMM
2000
SWE_LSU_1
1
V/V
0
SWE_INDO_3
1
V/V
0
SWE_SIM_3
1
V/V
0
SWT_ARCH_1
1
V/V
0

Well G

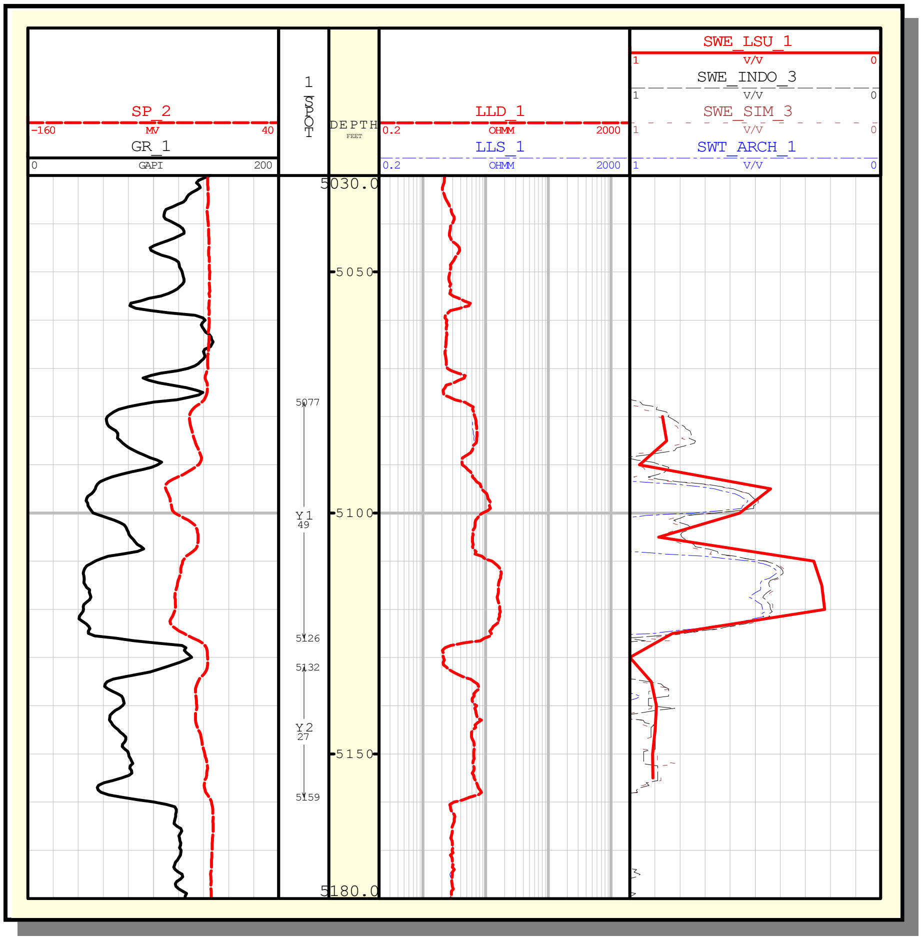

SP_2
-160
MV
40
GR_1
0
GAPI
200
1
TOPS
DEPTH
FEET
LLD_1
0.2
OHMM
2000
LLS_1
0.2
OHMM
2000
SWE_LSU_1
1
V/V
0
SWE_INDO_3
1
V/V
0
SWE_SIM_3
1
V/V
0
SWT_ARCH_1
1
V/V
0
5030.0
5050
5077
Y1
49
5100
5126
5132
Y2
27
5150
5159
5180.0

Well H

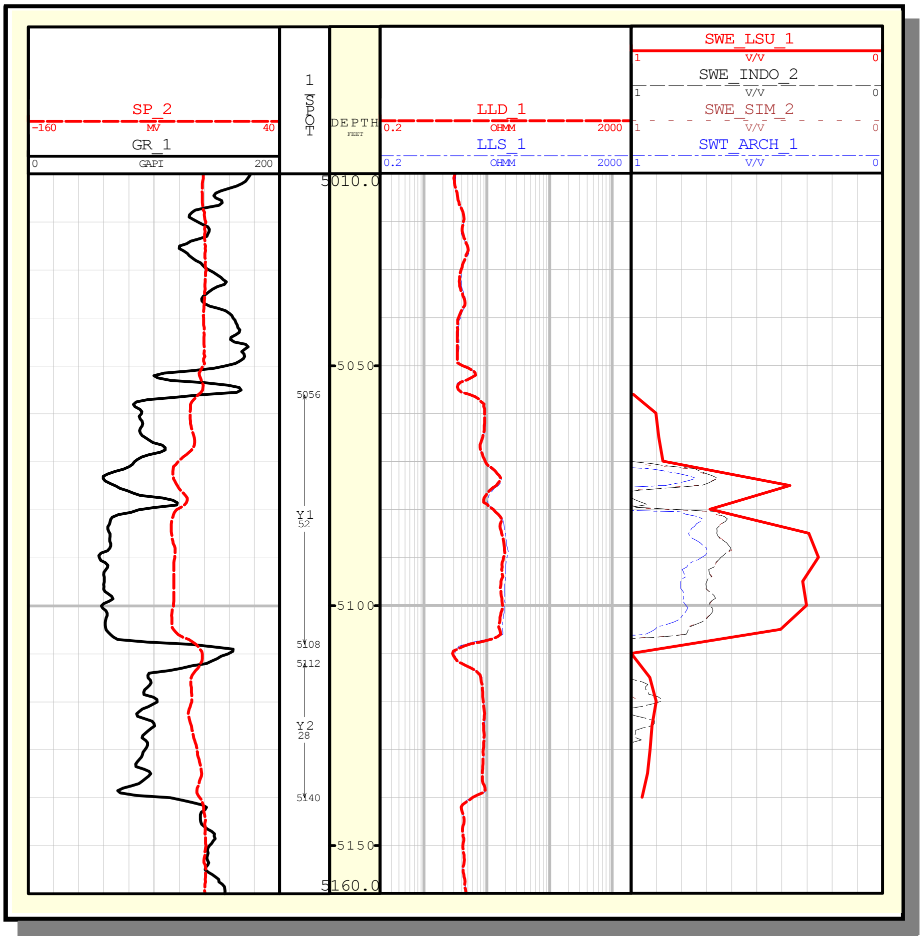
SP_2
-160
MV
40
GR_1
0
GAPI
200
TOPS_1
DEPTH
FEET
LLD_1
0.2
OHMM
2000
LLS_1
0.2
OHMM
2000
SWE_LSU_1
1
V/V
0
SWE_INDO_2
1
V/V
0
SWE_SIM_2
1
V/V
0
SWT_ARCH_1
1
V/V
0
5010.0
5050
5100
5150
5160.0
5056
Y1
52
5108
5112
Y2
28
5140

Well I

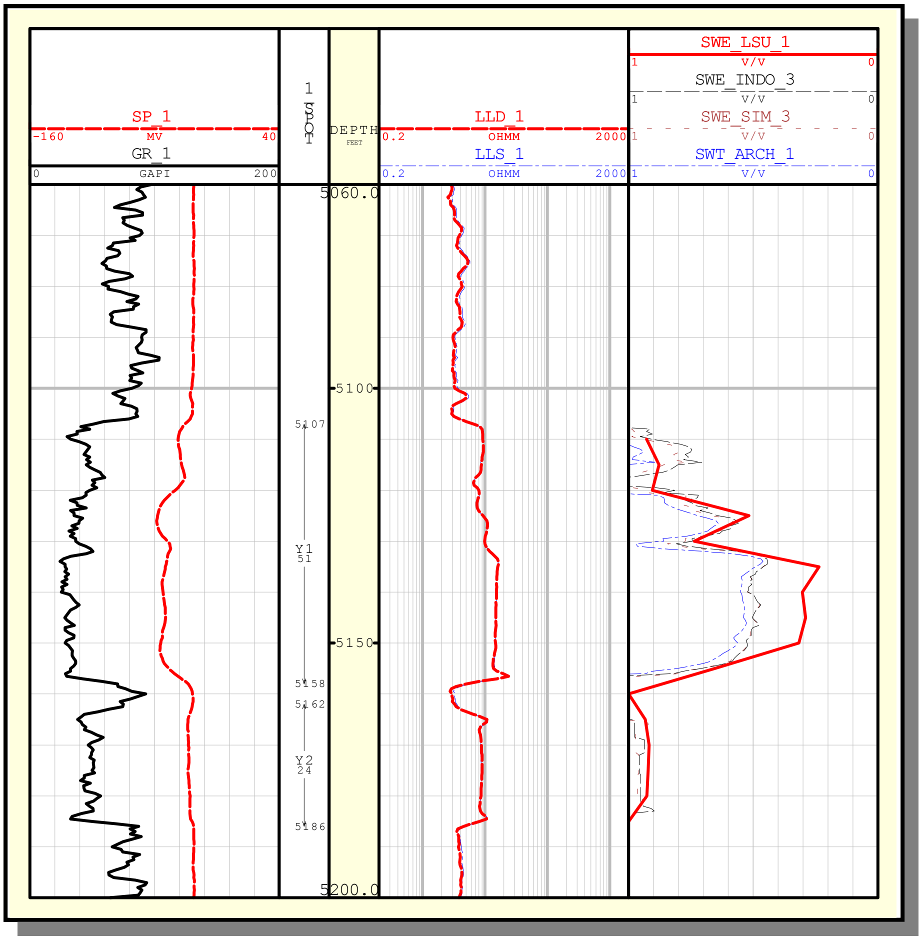

SP_1
-160
MV
40
GR_1
0
GAPI
200
TOPS_1
DEPTH
FEET
LLD_1
0.2
OHMM
2000
LLS_1
0.2
OHMM
2000
SWE_LSU_1
1
V/V
0
SWE_INDO_3
1
V/V
0
SWE_SIM_3
1
V/V
0
SWT_ARCH_1
1
V/V
0
5060.0
5100
5150
5200.0
5107
Y1
51
5158
5162
Y2
24
5186

Well J

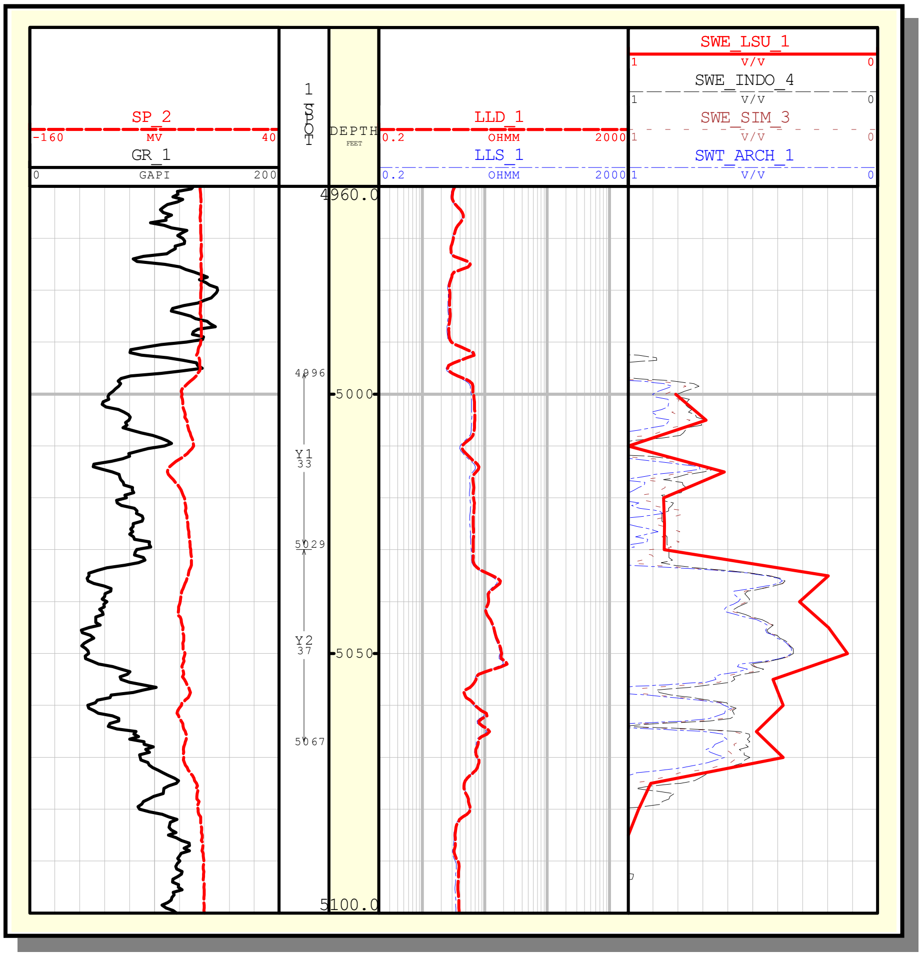

SP_2
-160
MV
40
GR_1
0
GAPI
200
1
SPOT
DEPTH
FEET
LLD_1
0.2
OHMM
2000
LLS_1
0.2
OHMM
2000
SWE_LSU_1
1
V/V
0
SWE_INDO_4
1
V/V
0
SWE_SIM_3
1
V/V
0
SWT_ARCH_1
1
V/V
0
4960.0
4996
5000
Y1
33
5029
Y2
37
5050
5067
5100.0

Well L

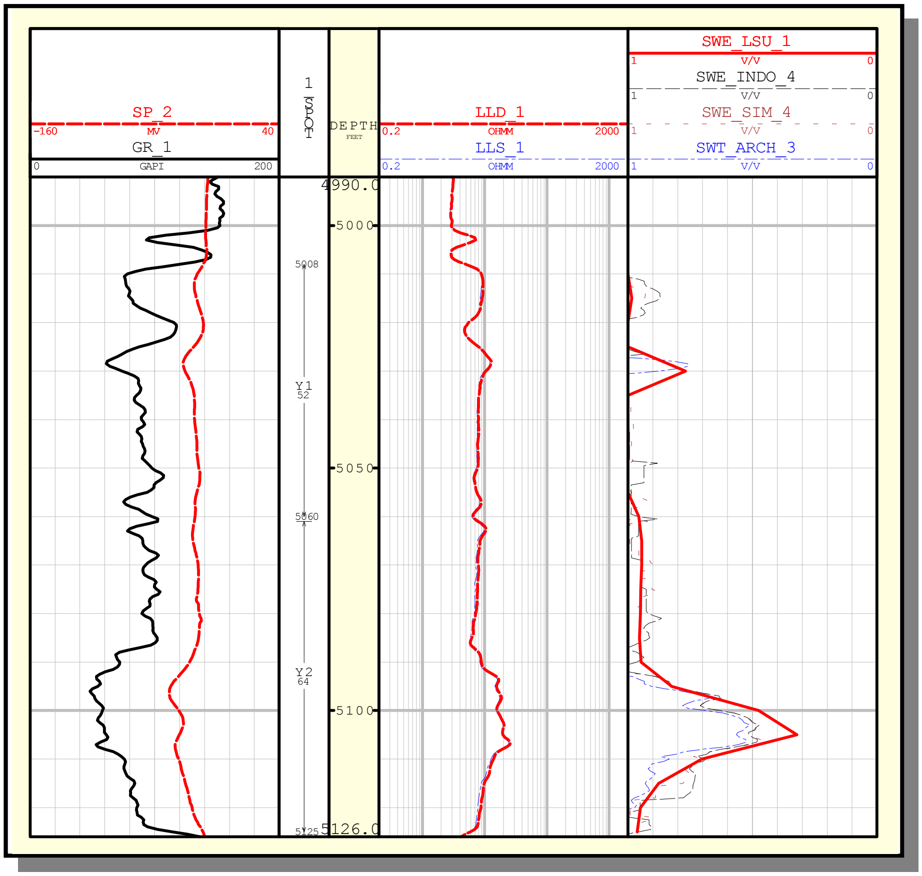
SP_2
-160
MV
40
GR_1
0
GAPI
200
DEPTH
FEET
LLD_1
0.2
OHMM
2000
LLS_1
0.2
OHMM
2000
SWE_LSU_1
1
V/V
0
SWE_INDO_4
1
V/V
0
SWE_SIM_4
1
V/V
0
SWT_ARCH_3
1
V/V
0
4990.0
5000
5008
Y1
52
5050
5060
Y2
64
5100
5125
5126.0

APPENDIX C

CORE DATA ANALYSIS: OIL AND WATER RELATIVE PERMEABILITY

Well B

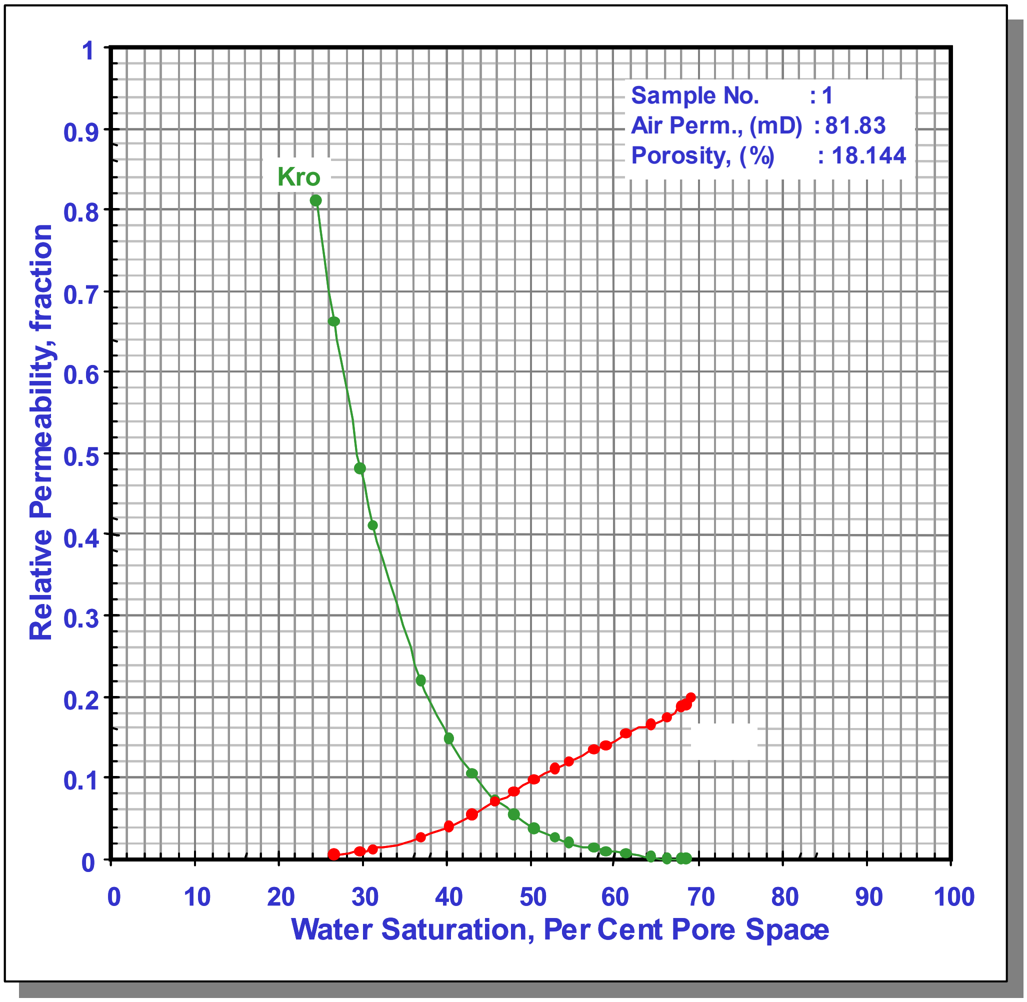
Sample No. : 1
Air Perm., (mD) : 81.83
Porosity, (%) : 18.144
Kro
Relative Permeability, fraction
1
0.9
0.8
0.7
0.6
0.5
0.4
0.3
0.2
0.1
0
0
10
20
30
40
50
60
70
80
90
100
Water Saturation, Per Cent Pore Space

Well B

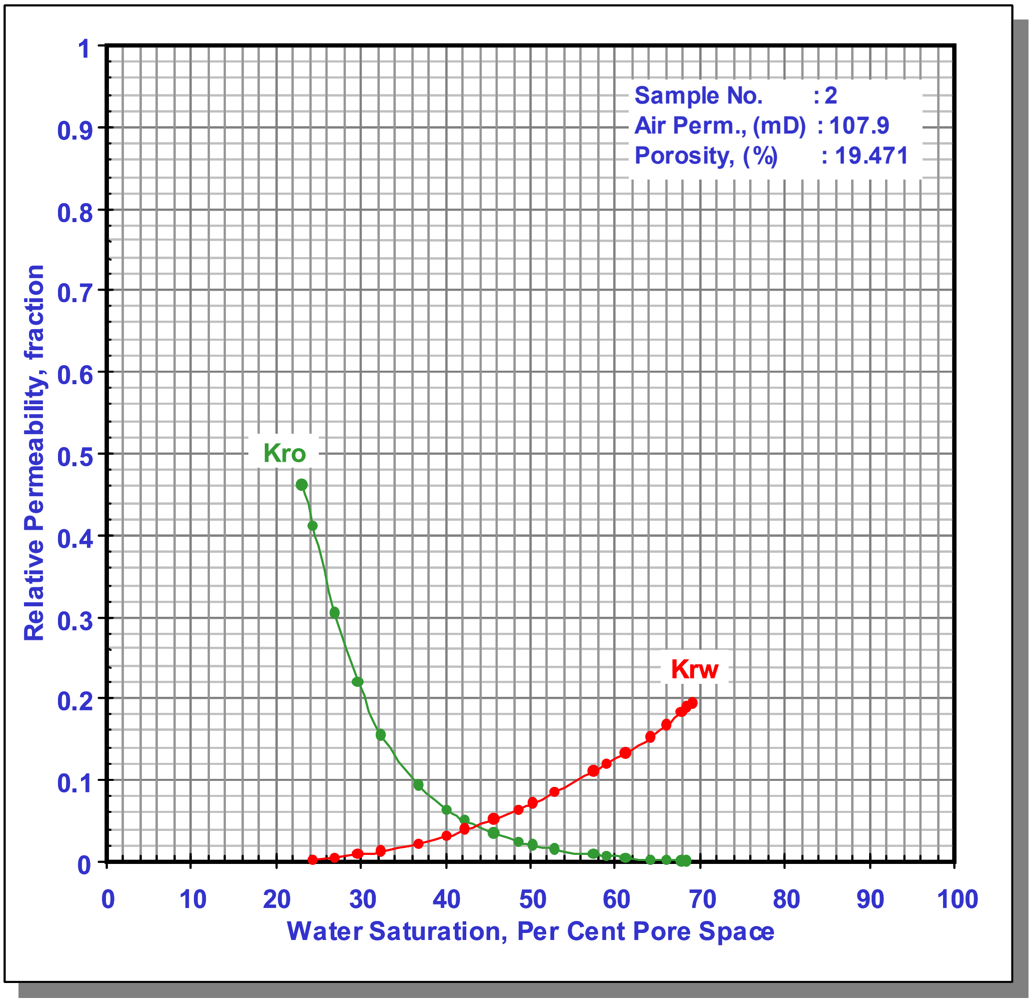
Sample No. : 2
Air Perm., (mD) : 107.9
Porosity, (%) : 19.471
Kro
Krw
Relative Permeability, fraction
Water Saturation, Per Cent Pore Space
0
0.1
0.2
0.3
0.4
0.5
0.6
0.7
0.8
0.9
1
0
10
20
30
40
50
60
70
80
90
100

Well B

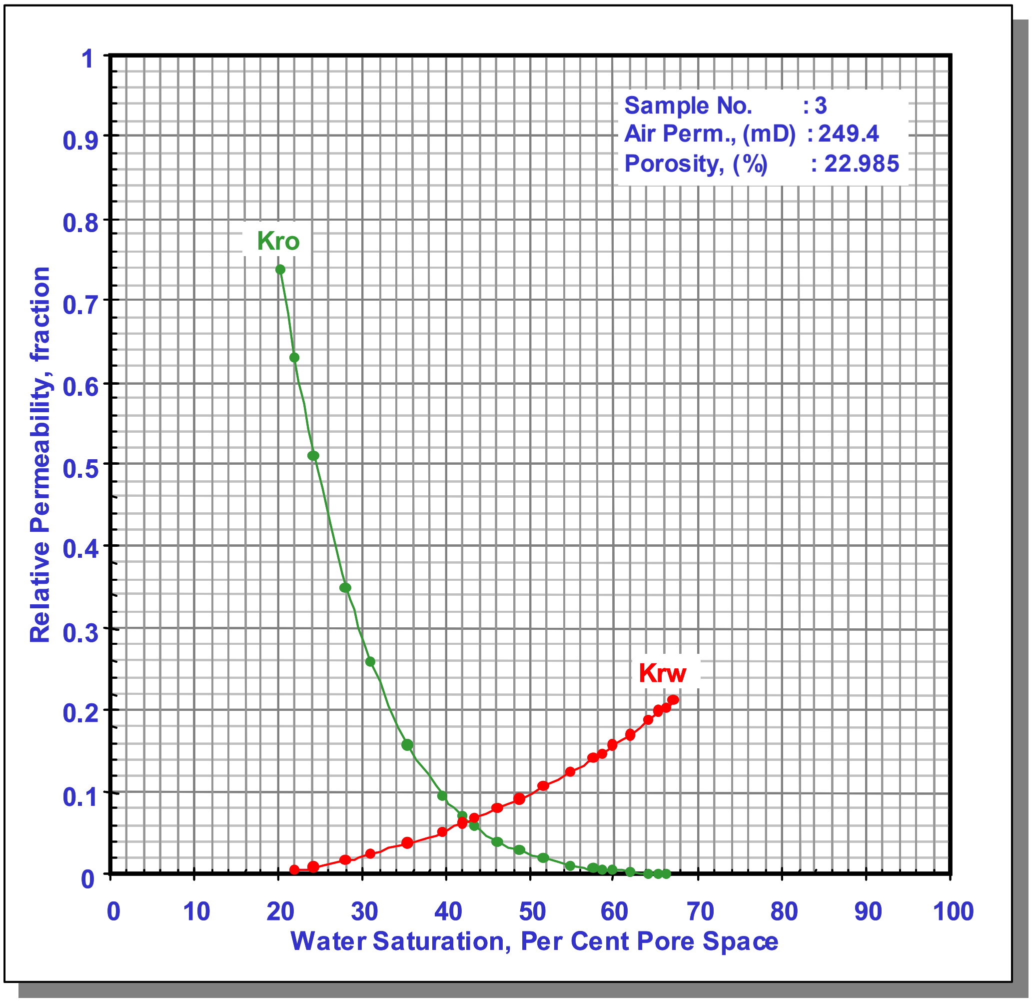

Sample No. : 3
Air Perm., (mD) : 249.4
Porosity, (%) : 22.985
Kro
Krw
Relative Permeability, fraction
1
0.9
0.8
0.7
0.6
0.5
0.4
0.3
0.2
0.1
0
0
10
20
30
40
50
60
70
80
90
100
Water Saturation, Per Cent Pore Space

Well K

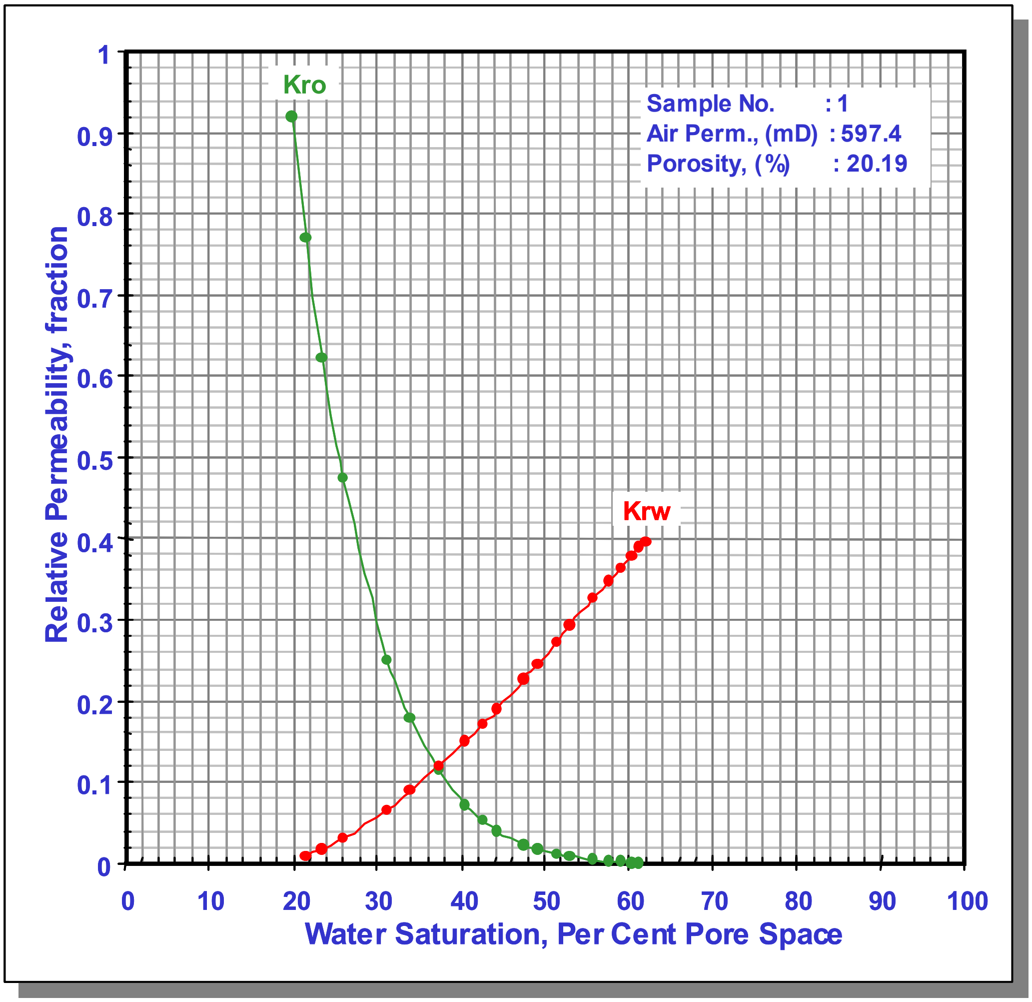
Kro
Krw
Sample No. : 1
Air Perm., (mD) : 597.4
Porosity, (%) : 20.19
Relative Permeability, fraction
1
0.9
0.8
0.7
0.6
0.5
0.4
0.3
0.2
0.1
0
0
10
20
30
40
50
60
70
80
90
100
Water Saturation, Per Cent Pore Space

Well L

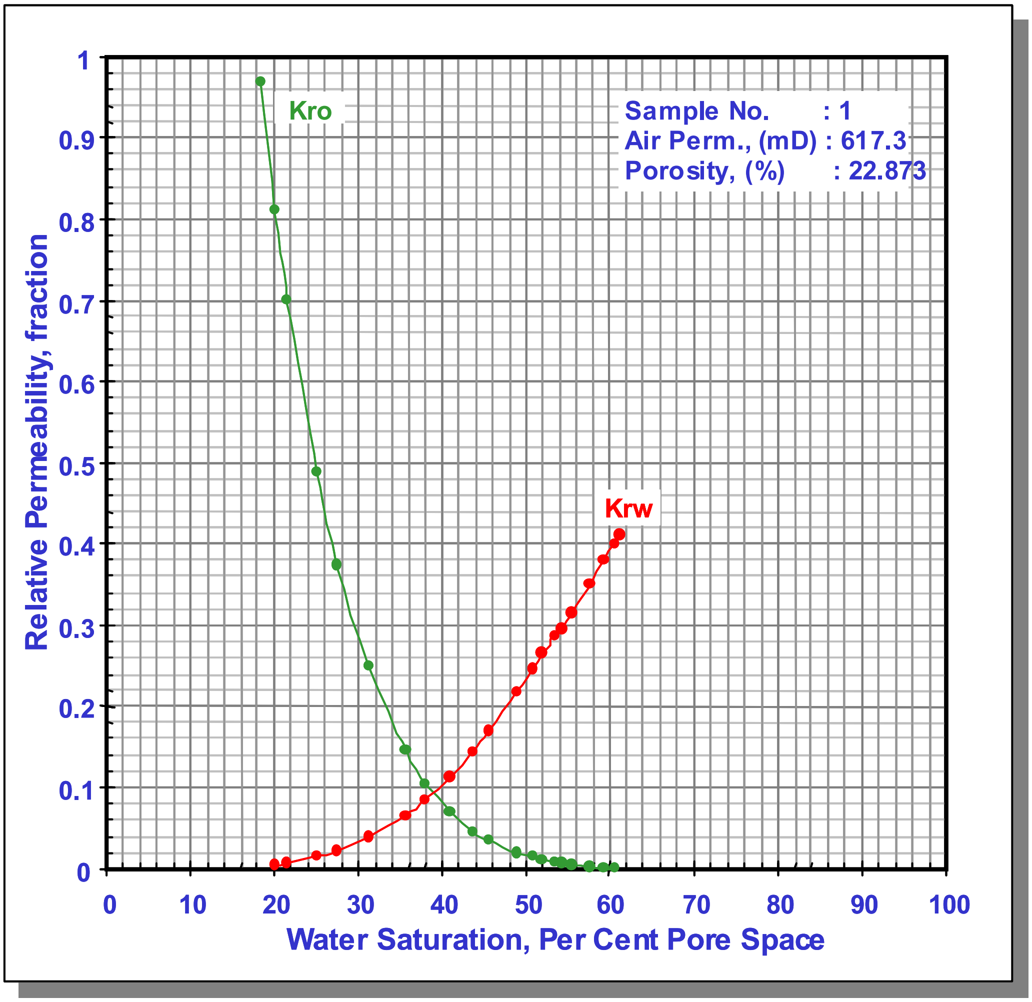

Kro
Krw
Sample No. : 1
Air Perm., (mD) : 617.3
Porosity, (%) : 22.873
Relative Permeability, fraction
1
0.9
0.8
0.7
0.6
0.5
0.4
0.3
0.2
0.1
0
0
10
20
30
40
50
60
70
80
90
100
Water Saturation, Per Cent Pore Space

APPENDIX D

CALCULATED WATER SATURATION DATA USING DIFFERENT MODELS

Well A

Depth	Indonesia	Simandoux	Archie	LSU
5089	1.000	1.000	1.000	0.980
5090	1.000	1.000	1.000	0.972
5095	1.000	1.000	1.000	0.968
5100	1.000	1.000	1.000	0.976
5105	1.000	1.000	1.000	0.955
5110	1.000	1.000	1.000	0.970
5115	0.928	1.000	1.000	0.968
5120	0.656	0.658	0.692	0.485
5125	0.715	0.717	0.752	0.571
5130	0.740	0.750	0.808	0.661
5135	0.797	0.810	0.865	0.754
5140	0.901	0.916	0.994	0.973
5145	1.000	1.000	1.000	0.988
5150	0.998	1.000	1.000	0.979
5155	0.975	0.996	1.000	0.975
5160	0.975	1.000	1.000	0.975
5164	1.000	1.000	1.000	0.983

Well B

Depth	Indonesia	Simandoux	Archie	LSU
4997	1.000	1.000	1.000	0.934
5000	0.983	1.000	1.000	0.920
5005	0.966	1.000	1.000	0.914
5010	1.000	1.000	1.000	0.939
5015	0.791	0.855	0.908	0.706
5020	1.000	1.000	1.000	0.927
5025	0.965	1.000	1.000	0.920
5030	0.989	1.000	1.000	0.922
5035	1.000	1.000	1.000	0.929
5040	0.638	0.629	0.668	0.460
5045	0.389	0.366	0.372	0.158
5050	0.597	0.570	0.666	0.442
5055	0.904	0.923	1.000	0.943
5060	0.538	0.514	0.530	0.311
5065	0.580	0.552	0.562	0.358
5070	0.820	0.822	0.941	0.850

Well C

Depth	Indonesia	Simandoux	Archie	LSU
5043	1.000	1.000	1.000	0.973
5045	0.941	0.899	1.000	0.966
5050	0.980	0.932	1.000	0.957
5055	1.000	0.880	1.000	0.976
5060	0.680	0.647	0.747	0.496
5065	0.926	0.852	1.000	0.969
5070	0.982	0.911	1.000	0.968
5075	0.629	0.601	0.677	0.409
5080	0.589	0.557	0.627	0.346
5085	0.574	0.543	0.612	0.330
5090	0.617	0.586	0.661	0.384
5095	1.000	0.858	1.000	0.969

Well D

Depth	Indonesia	Simandoux	Archie	LSU
5090	0.960	1.000	1.000	0.963
5095	0.850	0.936	1.000	0.945
5100	0.944	1.000	1.000	0.945
5105	0.770	0.830	0.886	0.735
5110	0.636	0.644	0.720	0.493
5115	0.648	0.651	0.746	0.529
5120	0.646	0.651	0.740	0.522
5125	0.642	0.650	0.732	0.511
5130	0.643	0.650	0.730	0.508
5135	0.851	0.935	1.000	0.913
5140	1.000	1.000	1.000	1.000
5145	0.953	0.942	1.000	0.971
5150	0.976	1.000	1.000	0.971
5155	0.975	0.945	1.000	0.971
5160	0.987	1.000	1.000	0.971
5165	0.946	1.000	1.000	0.970
5170	0.805	0.811	0.925	0.805
5175	0.475	0.455	0.507	0.250
5180	0.541	0.497	0.655	0.419

Well E

Depth	Indonesia	Simandoux	Archie	LSU
5035	1.000	1.000	1.000	0.896
5040	1.000	1.000	1.000	0.922
5045	1.000	1.000	1.000	0.959
5050	0.867	0.989	1.000	0.816
5055	0.991	1.000	1.000	0.893
5060	1.000	1.000	1.000	0.877
5065	0.953	1.000	1.000	0.875
5070	1.000	1.000	1.000	0.896
5075	0.995	1.000	1.000	0.806
5080	1.000	1.000	1.000	0.939
5085	1.000	1.000	1.000	0.930
5090	0.983	1.000	1.000	0.919
5095	0.949	1.000	1.000	0.919
5100	0.972	1.000	1.000	0.926
5105	0.926	1.000	1.000	0.930
5110	1.000	1.000	1.000	0.946
5115	1.000	1.000	1.000	0.866
5120	0.863	0.935	1.000	0.639
5125	0.994	1.000	1.000	0.919
5130	0.806	0.838	0.957	0.419
5135	0.479	0.476	0.489	0.190
5140	0.890	1.000	1.000	0.942

Well F

Depth	Indonesia	Simandoux	Archie	LSU
5032	1.000	1.000	1.000	0.985
5035	0.993	0.996	1.000	0.932
5040	0.976	0.975	1.000	0.945
5045	1.000	1.000	1.000	0.971
5050	1.000	1.000	1.000	0.973
5055	0.978	0.939	1.000	0.923
5060	0.980	1.000	1.000	0.932
5065	0.985	1.000	1.000	0.936
5070	0.982	0.961	1.000	0.924
5075	1.000	1.000	1.000	0.861
5080	1.000	1.000	1.000	1.000
5085	0.907	1.000	1.000	0.949
5090	1.000	1.000	1.000	0.985
5095	0.648	0.655	0.678	0.470
5100	0.629	0.643	0.668	0.459
5105	0.696	0.716	0.742	0.562
5110	0.751	0.778	0.811	0.670
5115	0.723	0.742	0.766	0.600
5120	0.727	0.744	0.767	0.601
5125	0.770	0.780	0.839	0.719
5130	0.911	0.947	1.000	0.948

Well G

Depth	Indonesia	Simandoux	Archie	LSU
5080	0.848	0.888	1.000	0.870
5085	0.739	0.768	1.000	0.853
5090	0.875	1.000	1.000	0.962
5095	0.586	0.592	0.661	0.439
5100	0.660	0.665	0.747	0.562
5105	0.792	0.844	1.000	0.885
5110	0.459	0.452	0.515	0.267
5115	0.445	0.434	0.482	0.234
5120	0.439	0.428	0.471	0.223
5125	0.785	0.765	0.907	0.830
5130	1.000	1.000	1.000	1.000
5135	0.924	0.969	1.000	0.914
5140	0.926	0.915	1.000	0.894
5145	0.916	0.914	1.000	0.899
5150	0.945	0.890	1.000	0.909
5155	0.889	0.876	1.000	0.908

Well H

Depth	Indonesia	Simandoux	Archie	LSU
5056	1.000	1.000	1.000	0.993
5060	1.000	1.000	1.000	0.902
5065	1.000	1.000	1.000	0.890
5070	1.000	1.000	0.977	0.874
5075	0.720	0.734	0.860	0.369
5080	0.837	0.865	1.000	0.687
5085	0.660	0.659	0.764	0.293
5090	0.643	0.640	0.713	0.255
5095	0.700	0.700	0.797	0.318
5100	0.689	0.687	0.777	0.302
5105	0.773	0.776	0.902	0.405
5110	1.000	1.000	1.000	1.000
5115	1.000	1.000	1.000	0.926
5120	0.881	0.981	1.000	0.901
5125	0.913	1.000	1.000	0.918
5130	1.000	1.000	1.000	0.925
5135	1.000	1.000	1.000	0.935
5140	1.000	1.000	1.000	0.957

Well I

Depth	Indonesia	Simandoux	Archie	LSU
5110	0.906	0.942	1.000	0.927
5115	0.801	0.859	1.000	0.877
5120	0.814	0.886	1.000	0.904
5125	0.643	0.665	0.710	0.517
5130	0.744	0.772	0.852	0.737
5135	0.460	0.460	0.480	0.236
5140	0.522	0.523	0.543	0.303
5145	0.504	0.506	0.529	0.290
5150	0.525	0.527	0.553	0.317
5155	0.711	0.718	0.800	0.655
5160	1.000	1.000	1.000	1.000
5165	0.987	1.000	1.000	0.932
5170	0.935	0.972	1.000	0.917
5175	0.956	0.958	1.000	0.921
5180	0.951	0.963	1.000	0.926
5185	1.000	1.000	1.000	1.000

Well J

Depth	Indonesia	Simandoux	Archie	LSU
5000	0.804	0.851	0.896	0.809
5005	0.689	0.752	0.815	0.687
5010	1.000	1.000	1.000	1.000
5015	0.698	0.736	0.773	0.614
5020	0.855	0.946	1.000	0.858
5025	0.804	0.898	1.000	0.854
5030	0.815	0.918	1.000	0.855
5035	0.432	0.434	0.438	0.198
5040	0.515	0.525	0.543	0.313
5045	0.431	0.432	0.436	0.196
5050	0.337	0.337	0.339	0.120
5055	0.573	0.607	0.629	0.420
5060	0.599	0.606	0.611	0.379
5065	0.555	0.577	0.660	0.486
5070	0.511	0.553	0.583	0.378
5075	0.791	0.998	1.000	0.909
5080	1.000	1.000	1.000	0.959
5085	1.000	1.000	1.000	1.000

Well K

Depth	Indonesia	Simandoux	Archie	LSU
5010	1.000	1.000	1.000	1.000
5015	0.870	0.932	1.000	0.984
5020	1.000	1.000	1.000	1.000
5025	1.000	1.000	1.000	1.000
5030	1.000	1.000	1.000	0.769
5035	0.916	1.000	1.000	1.000
5040	1.000	0.989	1.000	1.000
5045	0.993	0.986	1.000	0.999
5050	0.936	1.000	1.000	1.000
5055	0.987	0.984	1.000	1.000
5060	0.959	1.000	1.000	0.956
5065	0.986	0.992	1.000	0.944
5070	0.949	0.893	1.000	0.945
5075	0.927	0.903	1.000	0.948
5080	0.919	1.000	1.000	0.950
5085	0.912	1.000	1.000	0.954
5090	0.963	1.000	1.000	0.947
5095	0.820	0.820	0.901	0.824
5100	0.630	0.632	0.677	0.475
5105	0.515	0.510	0.551	0.321
5110	0.686	0.692	0.822	0.703
5115	0.737	0.779	0.925	0.876
5120	0.951	0.966	0.973	0.950
5125	0.959	1.000	1.000	0.963

VITA

(Bobby) Kurniawan was born in Jambi City, Indonesia, in July 18, 1973. In October 1996, he received a degree of Bachelor of Science in Geology from the Institute of Technology Bandung, Indonesia. In December 1996, he joined Schlumberger Oilfield Services as a field engineer and was assigned to Japan and Thailand. In March 1998, he accepted a job as a development geologist with Caltex Pacific Indonesia, a major oil company operating in Indonesia. In January 2001, he joined the Craft & Hawkins Petroleum Engineering Department at Louisiana State University to work towards a Master of Science degree in petroleum engineering. He is a member of Pi Epsilon Tau, the Society of Petroleum Engineers, and Indonesian Geologist Association.